FINAL REPORT

FFG Project number	854036	eCall number	6199094
Short title	ULE-Cavity-Access	Applicant	Institute for Quantum Optics and Quantum Information - Vienna
Consecutive number of the report	3	Reporting period	01.04.2016 to 30.09.2020
Author	Rainer Kaltenbaek		

1. Goals and results

In the following, I will describe all the core challenges we intended to meet, and the goals/objectives we laid out in the proposal to address these challenges. After describing these challenges and goals, I will describe for each of the goals: (1) if we achieved it, (2) if the goal was realistic, (3) what challenges and problems we encountered, and (4) which changes we had to make to meet these challenges. After that, we will provide some highlights we encountered during the project.

In the 2010 and the 2015 proposals of the medium-sized mission MAQRO [1,2], we defined a simple, setup for the central optical bench of MAQRO that was to operate at operating at cryogenic. Its core element was a high-finesse cavity, and we intended to couple light from into and out of the cavity using fixedly bonded fibre-mounted assemblies (FMAs) similar to the designs used for LISA Pathfinder and LISA using hydroxide-catalysis bonding [3,4]. While this has proved to be a very successful approach for LISA Pathfinder, the technique has never been used to implement a high-finesse optical cavity – neither at room temperature nor at the cryogenic operating temperatures of MAQRO.

The **core challenges** we wanted to address were:

(a) Bonding cavity mirrors with a sufficient accuracy such that one can find a stable, fundamental cavity mode.

(b) Aligning the cavity at room temperature such that it will operate at cryogenic temperatures.

(c) Integrating the cavity setup with FMAs to allow fibre coupling into the cavity mode.

(d) Analysing and reducing thermal stress that may occur on the optical bench of MAQRO because there will be various optical elements of various materials. When the optical bench is operated at different temperatures, thermal stress may occur.

In order to meet these challenges, the original proposal of ULE-Cavity-Access described the following **goals**:

(1) Define a finite-element model of the optical bench of MAQRO.

In order to design the optical cavity setup and the optical bench of MAQRO such that the cavity setup will be able to operate at room temperature and at cryogenic temperatures, and in order to avoid thermal stress, we planned to implement a thermal and structural model of the optical bench using the COMSOL software suite for finite-element simulation.

(2) Finite-element simulation of the optical bench to analyse thermally induced stress.

The optical bench of MAQRO will be assembled at room temperature, and it will later be cooled to a

cryogenic temperature around 20K during commissioning. Using a COMSOL finite-element model, the goal is to analyse the occurrence of thermal stress on the optical bench if the ambient temperature changes.

(3) **Position optical elements and choose materials to minimize thermally induced stress.**
The goal is to investigate possible changes in the geometry of the optical cavity and of the optical bench, and to choose an appropriate combination of materials in order to reduce thermal stress that may occur when operating the optical bench at different ambient temperatures. A good design of the optical bench geometry and good choices of the materials used will also help ensuring a good stability of the performance of the optical setup in the presence of temperature fluctuations.

(4) **Study smaller optical assemblies as precursors of studying the full optical-bench setup.**
As a precursor of improving the layout of the full optical bench of MAQRO, ULE-Cavity-Access aimed to initially study parts of the full setups. For example, this we envisioned to study initially study smaller-scale cavity assemblies consisting only of the cavity mirrors, or to study only the fibre-mounted assemblies. We also intended to study different ways of adhesively bonding optical elements – for example, by studying how different distributions of glue “spots” or different amounts of glue would affect the overall resilience of the assembly against thermal stress.

(5) **Adhesively bond a fibre-coupled test setup.**
In the proposal, we envisioned to separately adhesively bond a fibre-mounted assembly, the cavity mirrors and a lens to couple light from the fibres into (and out of) the optical cavity formed by the bonded mirrors.

(6) **Characterize the cavity at room temperature.**
After the assembly of the fibre-coupled test setup, the goal was to characterize the cavity and the coupling into and out of the cavity via the fibre-mounted assemblies. One of the goals was also to analyse the response of the test setup to temperature changes and to vibrations.

(7) **Characterize the cavity setup at cryogenic temperatures.**
After successfully performing the tests and the characterization at room temperature, the next step envisioned was to place the fibre-coupled test setup into a cryostat, and to test the performance of the setup at cryogenic temperatures.

(8) **Check whether the cavity setup survives repeated cooling to cryogenic temperatures.**
Apart from analysing the performance of the setup at room temperature and at cryogenic temperatures, another goal was to see whether the setup would survive repeated heating and cooling, and what the performance of the test setup would be while changing the ambient temperature.

While aiming to achieve the goals outlined above, we encountered multiple **challenges**. In the following, we will describe what these challenges were and how we tried to overcome them:

i. <u>Finding and acquiring appropriate adhesives.</u>
We knew from our sub-contractor ZARM Technik AG that the adhesives Hysol 9361 and Hysol 9313 would be suitable for space-ready optical assemblies operating at room temperature. During an earlier FFG project (MAQROsteps), we had used both adhesives successfully to bond cavities at room

temperature. Hysol 9313 is nearly transparent and has very low viscosity, such that it is suitable for the adhesive bonding of surfaces. Hysol 9361 is dark grey and has a very high viscosity, making it suitable for bonding optical elements using properly placed small “spots” of adhesive. For the present project, we faced multiple challenges regarding these adhesives. (a) only Hysol 9313 was readily available, while it was difficult to find a supplier of Hysol 9361. (b) only Hysol 9361 was specified to work at cryogenic temperatures as well as at room temperature. (c) when using Hysol 9313 for adhesively bonding surfaces, it was not clear how good the thermal contact would be, and (d) it was not clear how thick precisely the layer of the adhesive would be. We could resolve challenge (a) by getting access to Hysol 9361 via our sub-contractor ZARM Technik AG. In particular, they sent us an ample supply of the adhesive free of charge as part of our collaboration with them. In addition, we found an alternative adhesive (EP21TCHT-1) from the company Masterbond Inc that was certified by NASA to work in space environments, that had high viscosity for allowing adhesive bonding using “spots” of adhesive, and that was specified to work at cryogenic temperatures. Masterbond Inc. also offered a nearly transparent and low-viscosity adhesive (EP29LPSP) that was also NASA-certified for use in space environments and at cryogenic temperatures. This presented a solution for challenge (b). We met challenges (c) and (d) by deciding that we would not adhesively bond surfaces but to also use “spots” of high-viscosity adhesive. An alternative way to address challenges (c) and (d) would have been to mix micro-particles of known size and good thermal conductivity into the EP29LPSP adhesive. The disadvantage of that approach would have been that it can only be used for parts of the adhesive bonds required. For example, the cavity mirrors could only be safely bonded using “spots” of high-viscosity adhesive to avoid damaging the cavity mirrors. That was a lesson learned from our earlier FFG project MAQROsteps.

ii. Fitting the cavity setup and the fibre-coupling setup to the size of the MAQRO optical bench.

In the original proposal of ULE-Cavity-Access and in earlier designs of the optical bench of MAQRO, the idea was that the optical elements in the fibre-coupled cavity setup would all be along one line. That means, the light would exit from a fibre, be focused by a lens into the cavity, and then the light would be collected by a second lens after the cavity into another fibre. When we worked out the details of the setup, we found that it would be impossible to fit the cavity and the fibre-mounted assemblies on the optical bench of MAQRO that has the dimensions 20x20 cm^2. While we could, in principle, allowed for a slightly larger optical bench in MAQRO, the vacuum chamber we have available for testing the cavity setup does not allow a test setup longer than ~20cm. To overcome that challenge, we decided to design aspheric lenses that would allow keeping the dimensions of the setup within that size limit. During our thermal simulations, we saw that the only reliable way of mounting such aspheric lenses on the fused silica spacers we would use for the setup, would be for the lenses to also be made of the same material. Fitting fused-silica aspheric lenses were not available commercially. For that reason, we would have to design and acquire custom-made aspheric lenses made of fused silica. At the time of the last intermediate report of ULE-Cavity-Access, we had just finished designing the aspheric lenses necessary for that purpose.

iii. Changes in the optical beam due to temperature changes.

During the early phases of the project, we were mainly concerned with choosing the proper geometry and material for the lenses to avoid thermal stress or to keep that stress small. We also discussed that in the intermediate reports of ULE-Cavity-Access. Of particular concern was the design of the aspheric lenses. After finishing that design, we investigated how these lenses and the cavity setup would change if we cool down the setup from room temperature to cryogenic temperatures. These considerations showed that it is beneficial to use a SiC baseplate instead of Zerodur or fused silica in order to keep the changes to the cavity length small, and that the spacers should be of the same material as the aspheric lens. We could also see that the change to beam parameters like the waist and Rayleigh length would be ok, but the change in the refractive index of the lens material would lead to a significant shift of the position of the focused light. For that reason, we concluded that it would not be possible to use aspheric lenses for our fibre-coupled cavity setup. To meet this challenge, we had to adapt our setup to use aspheric, off-axis mirrors instead of aspheric lenses. The implications of this change were: (1) Instead of having a simple, 1D setup, we would have to design a 2D setup because the beam would have to be folded due to the reflections off the off-axis mirrors. (2) Our test setup would not fit within the cryostat available at ADS that we wanted to use for cryogenic testing. Due to point (1), we needed to devise a completely new design for the test setup. To meet the challenge resulting from point (2), we talked to colleagues at the Aspelmeyer group to see whether we could use one of their cryostats for the cryogenic tests to be performed in ULE-Cavity-Access. My colleagues agreed that I could use a cryostat one of them was building at that time. This had several advantages: (a) the cryostat was in Vienna, providing more direct access than we would have had if we had used a cryostat at the ADS premises in Germany. (b) We could test the setup down to 4K. Unfortunately, the self-made cryostat in the Aspelmeyer group turned out to have leaks, and before they were able to fix that issue, the person in charge left the Aspelmeyer group for a new position elsewhere. However, at that point, I agreed with the Aspelmeyer group that I would be able to use the 4K stage of their dilution refrigerator for our cryogenic tests. Apart from the already mentioned advantages, this had the additional advantage (c) that the 4K stage in the dilution refrigerator was much larger than our test setup, so that there would essentially not be any space limitations. (d) The dilution refrigerator operates at UHV pressures, such that we could not only test our setup and the adhesives at low temperatures but also under UHV conditions. (e) There were several optical fibres leading into the dilution refrigerator, and these fibres were identical to those that we planned to use for our test setup. This offered the possibility of simply splicing the fibres of our test setup to two of those pre-existing fibres in order to get optical access to our test setup at cryogenic temperatures.

iv. Acquiring custom-made aspheric optical elements.

We inquired with several companies to find suitable quotations for aspheric lenses. The prices quoted were well beyond the budget we had available (~40k€), and most companies we asked were not able to achieve the small radii of curvature we would have required for the aspheric lenses.

When we changed our design to use elliptical mirrors instead, the problems were similar, but we finally found one company that was able to supply elliptical mirrors to the specifications we needed for a price that we could afford with the budget available. Still, we only had enough budget to order two

elliptical mirrors. That was only sufficient for one fibre-coupled cavity setup, and we did not have any backup optical elements if any of the elements should be broken or damaged. Adhesively bonding optical elements already has the disadvantage that one can only try it once, and each bonding process is a potential point of failure. Having no backup elements meant that we had to be even more considerate at each step of the bonding process. This led to significant delays in the present project.

v. Material choices for the test setup.

As we indicated in point (iii), when we analysed how our cavity test setup would respond to changes in the ambient temperature, we found that (a) the spacers used for bonding the optical elements should be of the same material as the optical elements. That means, the spacers and the optical elements should all be made of fused silica. Because we already had cavity mirrors made from fused silica from the MAQROsteps project, and because the optical fibres are fused silica, we decided that the spacers for the optical elements then should also be fused silica. On the other hand, our analysis showed that SiC was a much better choice of material for the optical bench. A SiC optical bench is more thermally stable at cryogenic temperatures, and change of the cavity length as we cool to cryogenic temperatures is smaller for SiC than for fused silica.

vi. Using the dilution fridge of the Aspelmeyer group.

When we decided to perform some preliminary cryogenic tests, we encountered several practical issues in using the dilution refrigerator: (1) The vacuum pre-pump was broken. (2) Someone had removed the optical-access arms to the cold stage of the dilution fridge. That means, the fridge was open to atmospheric pressures. We could meet challenge (1) by using a small vacuum pre-pump I had bought for an earlier ESA-funded project. Thankfully, the pump was just strong enough to achieve the low pressure necessary to start the cryostat (several mbar). To meet challenge (2), we had to design and make vacuum flanges for the two openings in the dilution fridge.

vii. Aligning the optical elements with sufficient accuracy.

The key challenges in building an adhesively bonded cavity setup are: (a) Positioning the cavity mirrors accurately enough such that there is a cavity mode. (b) Making sure that these positions do not change while the adhesive cures. While we already did have some experience in this respect from the earlier FFG project MAQROsteps, the stakes were significantly higher this time. On the one hand, the procedure we used for MAQROsteps did rely on the accuracy of other, standard optical elements, and on the alignment of additional reference beams in a way that may have worked, but where added-up inaccuracies might lead to the failure of the whole process. On the other hand, while bonding the cavity mirrors was the final goal in MAQROsteps, it was only a first step in the present project. That means, a failure at this point would have meant a failure in the subsequent steps. Moreover, because MAQROsteps ended before we could fully characterize the bonded cavity, we do not know whether the procedure we used in that project actually produced the desired results. To this end, we devised a new approach for aligning the cavity mirrors that we thought to be more reliant. We continuously adapted and improved our alignment procedure in the course of the project, and we only bonded the second cavity mirror once we were very sure that we positioned it with the required accuracy. Because achieving the require accuracy was challenging, and because we did not have any backups in case

of a failure, we were very careful in this process. Unfortunately, this led to significant delays in finalizing the implementation of the cavity setup. In particular, while we already bonded the first cavity mirror in late January, 2019, it took us 18 months to be confident enough to bond the second cavity mirror in early August, 2020. The reason for this delay is that we tried many different approaches to make sure that the position of the second mirror would be correct within very small margins in its position and in its orientation. We will describe these procedures in more detail below.

viii. Finding the cavity mode.

One advantage of the procedures used in the final stages of finding the correct position for the second cavity mirror was that we already were scanning over cavity modes at that point. That means, we were already fairly certain that the input beam was close to the fundamental cavity mode. A significant challenge in this context was that we used a significant amount of infrared power for the input beam (50-100mW), and we used a significant amount of green laser light (40-100mW) to clearly see various back-reflections and to see light transmitted through the cavity. One of the alignment procedures we used often required changing the fibre connections between IR light and green light. Because of the high powers involved, dust on the fibre ends resulted in damaging several of the optical fibres used. Several times, that required exchanging the fibres, and that required realigning parts of the setup. Unfortunately, this resulted in delays in the final stages of the project in the summer of 2020 and, in particular, in finding the fundamental cavity mode.

Highlights:

The following list describe some of the highlights during this project:

- Switching the design of MAQRO from using aspheric lenses to couple light into the optical cavities to using aspheric off-axis mirrors. This change was an immediate success. Many of the challenges and the inaccuracies in designing aspheric lenses evaporated immediately when we switched to the mirror-based setup. In addition, while we did not find a company to manufacture the aspheric lenses we would have needed, we did find a good and reasonably priced supplier for the off-axis elliptical mirrors we then decided to buy.
- To do cryogenic tests using one of the dilution fridges of the Aspelmeyer group, we first had to close two gaping holes in the dilution fridge. Because the dilution fridge was custom made, we had to get a hand on the designs and then design two fitting vacuum flanges. We also had to find out from these designs which screws we would need. These were some very rare imperial screws we had to order. On top of that, we only had a very short time window for the cryogenic tests because Sungkun Hong from the Aspelmeyer group, who was the person in charge of the dilution fridge, was scheduled to leave for a new job soon after New Year 2018/2019. Moreover, the old dilution fridge makes so much vibrational noise that we could only operate it during times around Christmas 2018 while other experiments were dormant. Thankfully, Roland Blach from the workshop at the IQOQI quickly manufactured fitting flanges for us and saved Christmas 2018 for us.
- Unpacking the optical bench made from SiC and the off-axis elliptical mirrors was definitely a highlight.

A lot of thought, time and effort went into the corresponding designs and finding appropriate suppliers. It was very rewarding, finally, to hold these items in my hands.

2. Work packages and milestones

2.1 Synoptic tables

Table 1: Work packages (* - scheduled dates according to the original proposal)

WP No.	Work package title	Stage of completion	Scheduled date*		Current date		Results achieved / Deviations
			Start	End	Start	End	
1	Project Management	100%	03/16	02/19	04/16	09/20	The project management concluded as planned.
2	Local project management - ADS	100%	03/16	02/19	04/16	02/19	While I have been in contact with ADS, and they have been consulting me for some time during the project, they never signed a contract. After the retirement of U. Johann, there was a significant decrease in the interaction with ADS.
3	Local project management - ZARM	100%	03/16	02/19	04/16	03/19	The collaboration with ZARM was successful and worked as planned.
4	Design of cavities	100%	03/16	05/16	04/16	04/18	The design evolved considerably in the course of the project, in particular also significantly after the last intermediate report. This was necessary to make the design compatible with an operation at room temperature and at cryogenic temperatures. Designing the SiC baseplate and the elliptic mirrors took time and depended on results from WP9 and WP10.
5	Acquisition of components	100%	06/16	09/16	04/16	11/18	Delays due to the delays in WP4. Additional delays because the acquisition of the elliptical mirrors took half a year. These was a custom order for which the supplier had to update their milling equipment, achieving the required accuracy took a significant amount of time, and then the mirrors still had to be gold coated.
6	Implementation of cavities	70%	10/16	03/17	04/18	07/20	We successfully bonded the optical cavity, but the project ended before we could fully optimize and characterize the optical coupling and bond the optical elements for fibre coupling.
7	Characterization of cavities	20%	04/17	12/17	08/20	09/20	We could detect light transmitted through the bonded cavity, but optimizing the coupling into the cavity mode proved more challenging than anticipated, and the project ended before we could complete that task.
8	Cryogenic tests and characterization	25%	01/18	06/18	11/18	02/19	We performed cryogenic tests on parts of the setup. We tested several adhesives, and we tested gluing optical fibres into ferrules and the ferrules into ferrule holders. These tests were successful.
9	Definition of thermal model of optical bench	100%	06/16	09/16	04/16	10/17	We defined a thermal model of the cavity setup on our optical bench.
10	Thermal and structural simulation of optical bench	100%	07/18	02/19	06/18	11/18	We performed structural and thermal modelling of the prototype optical SiC bench we designed and ordered.

Table 2: Milestones (* - scheduled dates according to the original proposal)

Milestone No.	Milestone title	Scheduled date*	Current date	Milestone achieved on	Results achieved / Deviations
1	Critical review of cavity designs	06/16	03/18	03/18	We are confident that the cavity and baseplate design will fulfil the requirements of stable operation at room temperature and at cryogenic temperatures. The design should be space-proof in principle.
2	Critical review of components and of the optical-bench finite-element model.	10/16	02/19	02/19	The baseplate, the fused-silica spacers, ferrules, the elliptical mirrors and the flat mirrors fulfil the requirements. The finite-element model fulfilled the requirements for this project.
3	Critical review of adhesively bonded cavities	12/17	09/20	09/20	Cavity modes are visible in transmission through the bonded cavity, but we did not achieve fibre coupling into the fundamental cavity mode.
4	Critical review of adhesively bonded cavities with respect to performance in cryogenic environment	07/18	02/19	02/19	We could only test parts of the cavity setup at cryogenic temperatures.
5	Final review	02/19	09/20	09/20	We successfully designed an adhesively bonded, fibre-coupled high-finesse cavity using space-ready materials and bonding techniques. While we could successfully implement core parts of this design, we did not achieve fibre coupling into the fundamental cavity mode, and we therefore could not complete all tests planned.

Timescale (Plan/ Ist)

- Description of the gantt chart on the next page:
  blue bars and blue-shaded entries – durations and dates referring to contract/proposal

  orange bars and orange-shaded entries – durations and dates referring to actual status.

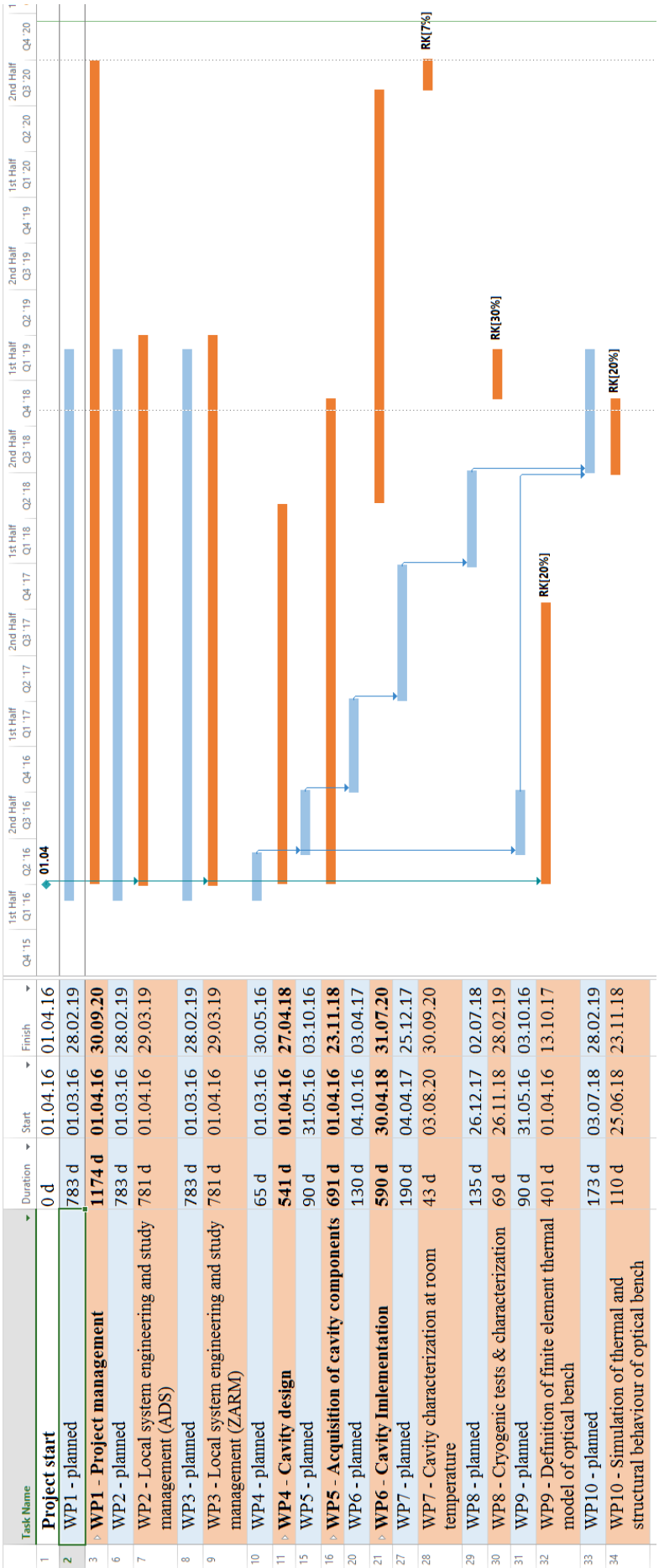

	Task Name	Duration	Start	Finish
1	**Project start**	0 d	01.04.16	01.04.16
2	WP1 - planned	783 d	01.03.16	28.02.19
3	**WP1 - Project management**	**1174 d**	**01.04.16**	**30.09.20**
6	WP2 - planned	783 d	01.03.16	28.02.19
7	WP2 - Local system engineering and study management (ADS)	781 d	01.04.16	29.03.19
8	WP3 - planned	783 d	01.03.16	28.02.19
9	WP3 - Local system engineering and study management (ZARM)	781 d	01.04.16	29.03.19
10	WP4 - planned	65 d	01.03.16	30.05.16
11	**WP4 - Cavity design**	**541 d**	**01.04.16**	**27.04.18**
15	WP5 - planned	90 d	31.05.16	03.10.16
16	**WP5 - Acquisition of cavity components**	**691 d**	**01.04.16**	**23.11.18**
20	WP6 - planned	130 d	04.10.16	03.04.17
21	**WP6 - Cavity Imlementation**	**590 d**	**30.04.18**	**31.07.20**
27	WP7 - planned	190 d	04.04.17	25.12.17
28	WP7 - Cavity characterization at room temperature	43 d	03.08.20	30.09.20
29	WP8 - planned	135 d	26.12.17	02.07.18
30	WP8 - Cryogenic tests & characterization	69 d	26.11.18	28.02.19
31	WP9 - planned	90 d	31.05.16	03.10.16
32	WP9 - Definition of finite element thermal model of optical bench	401 d	01.04.16	13.10.17
33	WP10 - planned	173 d	03.07.18	28.02.19
34	WP10 - Simulation of thermal and structural behaviour of optical bench	110 d	25.06.18	23.11.18

2.2 Description of the work carried out during the reporting period

Project management (WP1)

In this work package, we performed the overall project management as well as the local project management, first at the Faculty of Physics of the University of Vienna (UNIVIE), and later at the Institute for Quantum Optics and Quantum Information – Vienna, IQOQI-Vienna, of the Austrian Academy of Sciences. In autumn 2017, the project was moved from UNIVIE to IQOQI-Vienna. The project leader was initially employed at UNIVIE, and since October 2017, the project leader has been employed at the IQOQI-Vienna.

Another change was that the project leader got a position as an Associate Professor at the University of Ljubljana, starting in March 2019. Since then, the project leader's workload at the IQOQI-Vienna has been reduced to 20%. In January 2018, the project leader started to lead a second FFG-funded project (QuantumShield). Since March 2019, the workload of the project leader was equally distributed between QuantumShield (10%) and ULE-Cavity-Access (10%). We will discuss this in more detail in sections 2.3, 3, 5 and 7.

Local project management, Airbus Defence & Space (WP2)

This work package was for the local project management of our sub-contractor Airbus Defence & Space (ADS). Until the intermediary reports (reports 1 and 2 of this project), the collaboration with ADS and the local project management were proceeding as planned. In March 2018, however, Dr. Ulrich Johann, who had until then been our main contact at ADS, went into retirement. Following his retirement, our collaboration with ADS became less intense and our interactions became less frequent despite of efforts to establish a similarly good collaboration with Dr. Johann's successor at ADS. In particular, the PI was in contact with Dr. Domenico Gerardi, who was part of Dr. Johann's team and continued to work at ADS, and Dr. Gerardi introduced the PI to Dr. Ulrich's successor by during one of his visits with ADS in the early stages of the present project.

The scaling down of the collaboration with ADS did not have significant consequences for the present project. For example, the design of our cavity prototype setup evolved in such a way that it became clear in late 2017 and early 2018 that the setup would not fit into the cryostat at the ADS premises we had planned to use for the cryogenic tests in this project. Instead, we agreed with the Aspelmeyer group at UNIVIE to use one of their cryostats for our experiments.

In late 2018 or early 2019, we agreed with Domenico Giardini at ADS that they would not charge us for our collaboration. We communicated this to the FFG, and we used the budget that we had originally reserved for ADS for building our cavity prototype instead. This proved beneficial because the costs for the SiC baseplate and for the custom elliptical mirrors in the adapted prototype design exceeded the costs we had estimated originally. With the budget reallocation, we were able to cover the higher costs for the prototype with the project budget available.

Local project management, ZARM Technik AG (WP3)

The sub-contractor performed, and concluded this work package as planned. In particular, we had regular contact over the phone, and via e-mail, and T. Schuldt joined us for several days in Vienna in order to discuss and test the bonding of optical components with the adhesives we intended to test. Moreover, the sub-contractor sent us supplies of Hysol 9313 and Hysol 9361. In particular, the Hysol 9361 later turned out to be

one of the adhesives we chose for the actual implementation of our prototype cavity sestup.

The design of the cavity setup (WP4)

This work package often went hand in hand with work packages WP9 and WP10 (**WP9** – Definition of finite-element thermal model of optical bench, **WP10** – Simulation of thermal and structural behaviour of optical bench) because it often proved useful during the design phase to double-check the effects of temperature changes or of vibrations on the finite-element model.

It was clear from the beginning that it would be a considerable challenge in **WP4** that we would first have to assemble and characterize the cavities at room temperature before cooling the assembly down to the intended operating temperature at 20K or below. In the cool-down process, the various parts of the cavity setup may experience different thermal expansion due to several reasons: (a) it may occur if one uses different materials in building the assembly. (b) It will also occur in cases where parts of the setup cool down at different rates due to a lack of thermal conductivity in the interfaces between the elements. This renders it paramount to (1) use adhesive-bonding techniques that allow for good thermal conductivity, and (2) to use materials with identical or very similar thermal properties. We will discuss these issues in more detail in the context of WP10.

To address this challenge, we soon began to implement and to investigate finite-element models of the cavity setup to investigate the occurrence of thermal stress during the cool-down procedure. That means, we essentially began work on **Work Packages 9 and 10** (**WP9** – Definition of finite-element thermal model of optical bench, and **WP10** – Simulation of thermal and structural behaviour of optical bench) at the same time as our work on WP4. A central prerequisite for implementing such a finite-element model is to have good models for the materials used valid from cryogenic temperatures up to room temperature.

We intended to implement test cavities with a finesse of around 10^5. This corresponds to a full width at half max (FWHM) cavity linewidth of $2\kappa \simeq 10^5\ \mathrm{rad/s}$. For a 10cm long cavity, that means that any changes in cavity length, e.g., due to temperature changes, should be much less than half a micrometre. That corresponds to a relative change in cavity length of 1ppm or less. This is a very tight restriction on the material for the baseplate of the cavity. For an operating temperature around room temperature, Zerodur would be an adequate material for this purpose. For the cryogenic operating temperature we aim for (20K or less), we concluded early in the project that Silicon Carbide (SiC) would be better suited. We reported this conclusion already during the first reporting period.

That meant we needed a SiC baseplate while the optical elements would be made of highly transparent glass. In the context of space-based experiments, the material of choice typically is Fused Silica as in the case of LISA Pathfinder [5]. Reasons for this choice are the radiation hardness of Fused Silica as well as its low absorption at the design wavelength of 1064nm. The use of SiC as a baseplate for optical instruments has significant technological heritage from the GAIA mission [6].

For the GAIA mission, a novel type of SiC material was developed that can be polished to optical grade and that can be brought into arbitrary shapes. The GAIA mission harnessed SiC to realize the baseplate of the optical assembly as well as a large optical-grade mirror. These developments have led to the foundation of the companies Boostec and Optosic (now both part of the Mersen group), which specialize in the manufacture of SiC products.

During the early stages of the project, we assumed that we would use lenses to couple light into the cavity mode. We assumed that the material of these lenses would be borosilicate, fused silica or a comparable,

typical lens material. In any case, the lenses would be of a material different from SiC, which we assumed to be the optimal material for the baseplate. If one uses different materials, these would have different coefficients of thermal expansion, and that would have led to thermal stress when cooling the optical assembly from room temperature to a cryogenic operating temperature. We plan to minimize this effect by the following means:

- Keeping as much distance as possible between the location of interfaces between different materials and the location of optically sensitive areas (e.g. mirrors, lenses)
- Using adhesives with high thermal conductivity to minimize thermal stress during cool down
- Using tightly localized and tensile adhesive bonds for the interfaces between materials with different coefficients of thermal expansion (Hysol 9361 or similar)

At the time of the first intermediate report, we still needed to investigate the precise way of adhesively bonding components of different material more closely. In particular, we were not yet certain which adhesive we would use and whether we would apply the adhesive in well localize spots or if we would apply the adhesive over a thin but large area. This depends on the thermal stress that may appear if we adhesively bond components consisting of different materials or if there is not sufficient thermal conduction. It is not trivial to implement a finite-element model to analyse the thermal stress occurring in this context. For that reason, we will discuss this issue in the context of WP9.

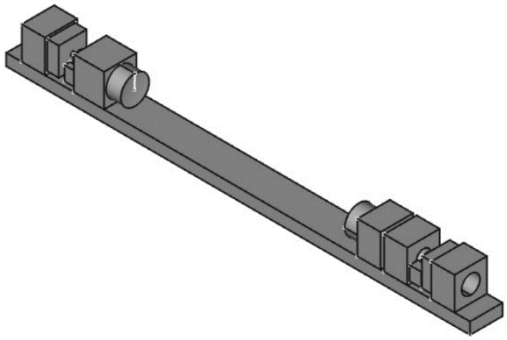

Figure 1: Preliminary CAD model of the cavity design from the first intermediary report. The cavity design is two sided with a fibre coupler on either end. In this early design, the fibre ferrule was mounted in a fused-silica spacer ($12 \times 12 \times 5$ mm^3) with a 1.8mm central hole. This "fibre-spacer" was mounted on a spacer with a much larger central hole to accommodate a fibre stress relief and to allow XY- alignment of the position of the fibre. The lens was mounted on a U-groove mounted on a spacer. That allowed full freedom in XYZ to adjust the position of the lens relative to the fibre. The mirrors were adhesively bonded to spacers as in our earlier FFG project MAQROsteps (Project No 840089).

When we wrote the second intermediate report for the project in October 2017, we were still sure we would build a 1D-cavity test setup using aspheric lenses to focus light into the cavity. In particular, we expected a design similar to the one illustrated in **Figure 1**. The reasoning behind this design was that (1) it would be similar to the design we developed for the earlier FFG project MAQROsteps (Project No 840089), and (2) the small transverse diameter of the design would allow mounting the cavity assembly in the cryostat at the premises of ADS we intended to use for the cryogenic tests.

One concern that we still had to address at that point was how to mount the optical assembly in the cryostat. In particular, we were concerned that the mounting could result in significant thermal stress. For that reason, we considered possible mounting options to minimize thermal stress. One attractive option was a method that

was used in the GAIA mission to mount fused-silica elements to a SiC baseplate. In particular, they used a clamping mechanism as illustrated in **Figure 2**. The figure is from the PhD thesis of M. van Veggel [7]. This mechanism allows for free thermal expansion perpendicular to the clamping direction. This way, no thermal stress builds up.

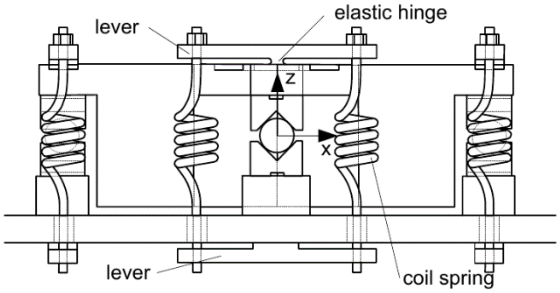

Figure 2: Beam-splitter mount used in GAIA to allow keeping optical alignment during cool down despite thermal expansion. The figure is from the PhD thesis of M. van Veggel, TU Eindhoven, 2007.

Between the first and the second intermediary reports, our work focused on designing the aspherical lenses we would need to focus light directly from the optical fibre assembly into the cavity mode such that the overall optical assembly would fit on an optical bench of 20cm. This size limitation was imposed by the design of the optical bench for MAQRO. In particular, the thermal shields for passive radiative cooling in the MAQRO mission design imposes a size limitation on the cold, experimental volume.

In order to minimize thermal stress, we had decided at that point that the best solution would be to use custom-made aspheric lenses made from fused silica. The standard aspheric lenses available commercially did not have the focal lengths that we required, and they consisted of materials where it would not be certain how they would behave under cryogenic conditions and what thermal stress may occur if we bond them to fused silica spacers at room temperature and then cool them down.

By using ray propagation and optimizing the optical delays between the fibre tips and the focal point inside the optical cavity, we found the optimal shape of the aspheric lenses we would need to couple light into and out of the cavity mode. The general shape for each of the aspheric lenses was:

$$f(r) = \frac{r^2}{R\left(1+\sqrt{1-\frac{r^2}{R^2}(1+k)}\right)} + \sum_{m=2}^{n} A_{2m} r^{2\,m} \qquad (1)$$

Here, R is the radius of curvature of the lens at $r = 0$, k is the conic constant, and A_m are constants, and r is the distance from the beam axis. All the constants were determined by a multi-parameter fit. To distinguish between the two lenses on opposing sides of the cavity assembly, we denoted the lens close to the cavity mirror with a radius of curvature of 75mm as F1, and we denoted the other lens as F2. For the parameters describing the shapes of the two aspheric lenses, we found:

$$R_{\mathrm{F1}} = 2.4945\mathrm{mm} \pm 0.5\mu\mathrm{m}$$

and

$$k_{\mathrm{F1}} = -2.0328 \pm 0.0014$$

The values and tolerances in the polynomial parameters for F1 were:

$$A_{4,F1} = (130 \pm 6) \times 10^{-6}\text{mm}^{-3},$$
$$A_{6,F1} = (-6.4 \pm 1.5) \times 10^{-6}\text{mm}^{-5},$$
$$A_{8,F1} = (3 \pm 4) \times 10^{-7}\text{mm}^{-7},$$
$$A_{10,F1} = (-1 \pm 10) \times 10^{-8}\text{mm}^{-9},$$

We determined the tolerances by requiring that the deviation of the resulting lens shape from the "ideal" lens shape over the size of the clear aperture is less than $\lambda/10$.

For F2, we got:

$$R_{F2} = 1.1874\text{mm} \pm 0.2\mu\text{m},$$
$$k_{F2} = -2.0181 \pm 0.0004$$
$$A_{4,F2} = (1416 \pm 7) \times 10^{-6}\text{mm}^{-3},$$
$$A_{6,F2} = (-292 \pm 2) \times 10^{-6}\text{mm}^{-5},$$
$$A_{8,F2} = (592 \pm 4) \times 10^{-7}\text{mm}^{-7},$$
$$A_{10,F2} = (-95 \pm 1) \times 10^{-7}\text{mm}^{-9},$$
$$A_{12,F2} = (107 \pm 3) \times 10^{-8}\text{mm}^{-11},$$
$$A_{14,F2} = (7 \pm 1) \times 10^{-8}\text{mm}^{-11}.$$

That means, when we submitted the second intermediary report, the designs for the aspheric lenses were essentially finished, but we spent the subsequent month double-checking the design of the aspheric lens for the cavity test setup. In the course of that, we noticed several issues with using aspheric lenses for our design:

- The tolerances on the parameters for the aspheric lenses were very small, which would make them extremely hard to manufacture.
- The radii of curvature were very small – again, a challenge for manufacturers.
- We tested the effects on the lens and the optical setup if one cooled it from room temperature to cryogenic temperatures. In our description of WP10, we will present the results of these considerations. They led to a crucial redesign of the test setup and the optical bench.

As we mentioned above, we already concluded in the first intermediate report that the optical elements and the spacers carrying them should ideally be of the same material (fused silica) in order to avoid thermal stress where possible (see WP9 and WP10). If the optical bench and all the optical elements were made from fused silica, then there would be no thermal stress except, potentially, at the mounting points of the bench.

We then investigated how our aspheric-lens design would be affected by changing the temperature. Because of the low thermal expansion of fused silica even over large changes of temperature, the shape of the lenses does not change much, and the focal length of lenses due to changes of the lens shape will be similarly small. While that seemed to be okay, the refractive index of glass will change with the temperature as well.
In order to define the shape of our aspheric lenses, we aimed to minimize the aberration in focusing a bundle of rays incident on the lens after originating from an earlier focal point. In our case, that would correspond to the light originating from a fibre and then being focused into the cavity. The problem then was the following: if we design the aspheric lens for an operation at room temperature, we get a slightly different shape than if we were designing it for an operation at cryogenic temperatures. While the changes to the shape were not large, the position of the resulting focus relative to the flat slide of the aspheric lens was significant. For example, if we designed the aspheric lens to focus into the cavity on the side with the 75mm radius of curvature mirror at room temperature, the focus at 20K would be nearly 10mm off. While that is smaller than the 36.6mm Rayleigh length of the beam exiting the cavity at that mirror, it is large compared to the 48µm Rayleigh length of the beam exiting the fibre. We therefore concluded that we would not risk such large shifts in the beam parameters between the design temperature and the operating temperature. That meant we **could not use (aspheric) lenses** in our setup. The same holds true for the optical-bench setup of MAQRO. For that reason, we decided to adapt our setup to use **off-axis elliptical mirrors** instead. The design faced and solved several challenges:

- Achieving the desired focal-point distances while at the same time keeping the radii of curvature of the mirrors sufficiently large to allow manufacturing these mirrors. In particular, the second elliptical mirror (eM2) was challenging in this respect.
- Defining the design in such terms that it would be clear to the manufacturer. This required several detailed e-mails and phone calls.
- One particularly important point was how to cut the elliptical mirror from the substrate. The symmetry axis for the cylindrical cut had to be parallel to the minor axis of the ellipsoid for each mirror.
- Unfortunately, a lot of the mirror substrate was wasted because we only could afford one mirror of each of the designs. Multiple mirrors would not have cost proportionally more because the milling and the coating would have been a common work step.
- Implementing the 3D CAD model for these mirrors was challenging because it took me some time to understand the symmetries one can use in the construction.
- We had to consider carefully how we would be able to align and adhesively bond these mirrors.
- Because we now had to fold the overall setup in 2D, it was clear that we would not be able to use the ADS cryostat. This was not an issue because: (a) we had access to cryostats in the Aspelmeyer group. (b) because the level of collaboration with ADS faded after the retirement of U. Johann we preferred not to be dependent on a cryostat at the ADS premises. (c) ADS did not ask for a payment despite our initial oral agreement. That freed up some budget for realizing the cavity assembly, which turned out to be more expensive than anticipated.

Figure 3 and **Figure 4** show the propagation of rays from the foci corresponding to the fibre tips via the elliptical mirrors eM1 and eM2 towards their foci inside the cavity. To keep these plots simple, the two foci in

each of these plots lie on the y-axis (the vertical line). Due to space considerations, we do not show the convergence of the rays into the foci inside the cavity.

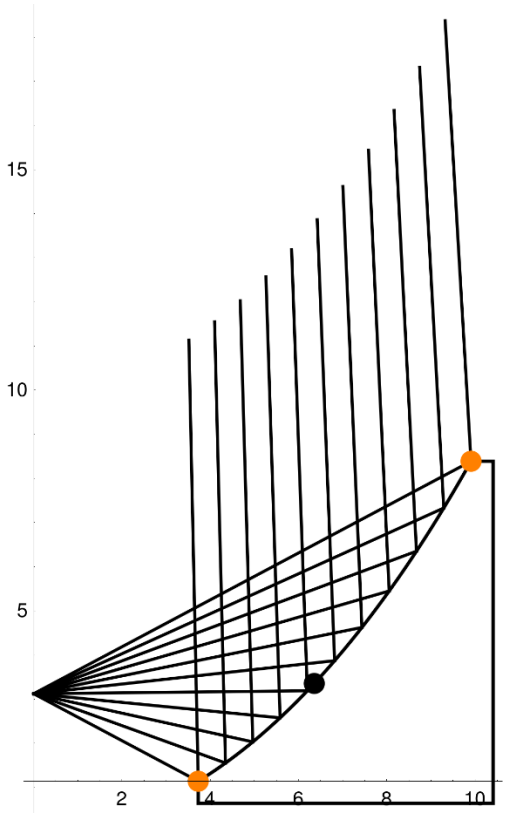

Figure 3: Ray propagation from fiber tip to focus inside cavity via elliptical mirror eM1. The orange dots indicate the mirror edges, the black dot the intersection with the horizontal ray.

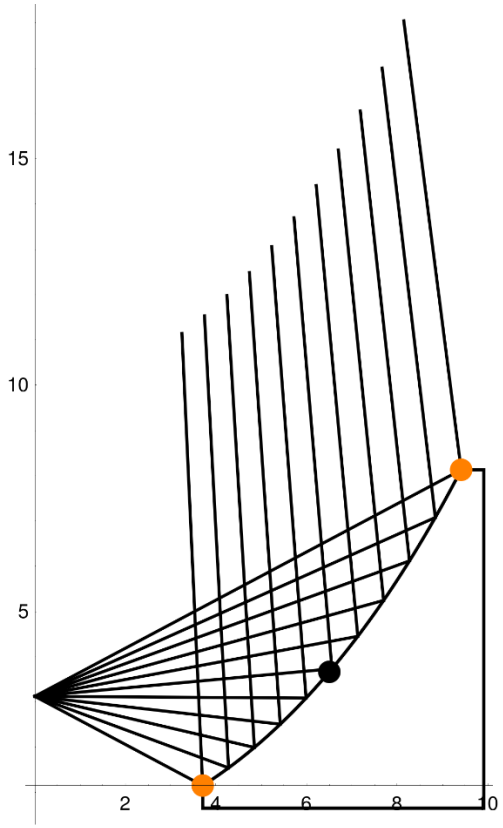

Figure 4: Ray propagation from fiber tip to focus inside cavity via elliptical mirror eM2. The orange dots indicate the mirror edges, the black dot the intersection with the horizontal ray.

Figure 5 and **Figure 6** show construction drawings for the two elliptical mirrors. The major and minor axes of eM1 are 90mm and 23.5mm, respectively. The distance between the two foci of eM1 is 173.8mm. For eM2, the major and minor axes of the ellipsoid are 42.5mm and 16mm, respectively, and the distance between the two foci is 78.7mm.

Both mirrors were manufactured from fused silica, and the ellipsoid surface was coated with unprotected gold in order to achieve reasonably high reflectivity while not altering the polarization of the reflected light. We chose gold in order to minimize the emission of thermal radiation from the reflective surface. The same coating was applied to two fused-silica blocks to later use them as flat mirrors for folding the beams. We had them shipped directly from the manufacturer of the fused-silica spacers (Lens Optics) to the manufacturer of the elliptical mirrors. They then had all of these items coated with (unprotected) gold.

Initially, we asked the same company we had contacted with respect to the aspheric lenses to manufacture these off-axis elliptical mirrors instead. This was not possible because that company at first asked us what our maximum budget was for this project. When I told them, they refused any further discussions. After contacting many potential alternative suppliers, I finally came across B-Con Engineering in Ontario, Canada. They agreed to make the mirrors for us, but they underestimated the effort. In particular, they had to buy new milling tools, and the milling itself took them weeks for each mirror. The mirrors themselves turned out well, but the overall

acquisition took more than half a year.

After we had designed the elliptical mirrors, the central question became what the optical bench should then look like, how we would position the optical elements on that optical bench, and how we would be able to align the different degrees of freedom of those optical elements.

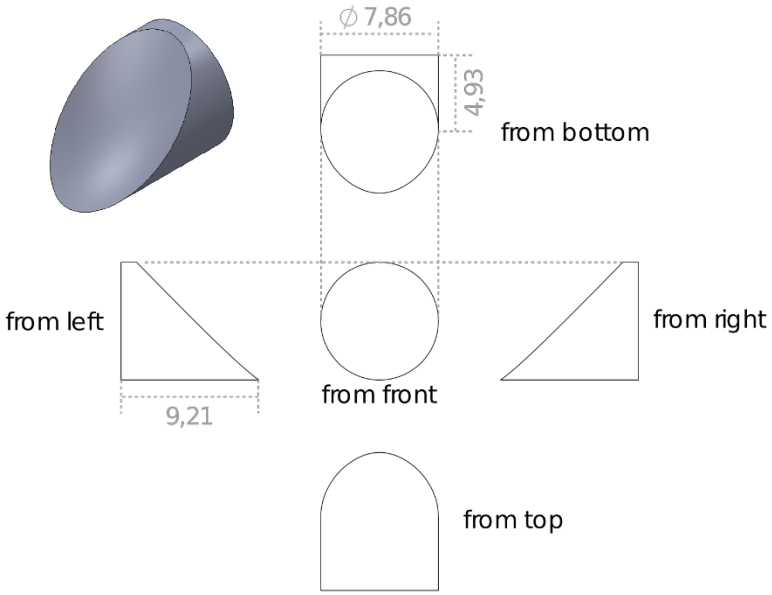

Figure 5: Construction drawing of elliptical mirror eM2. [dimensions in mm]

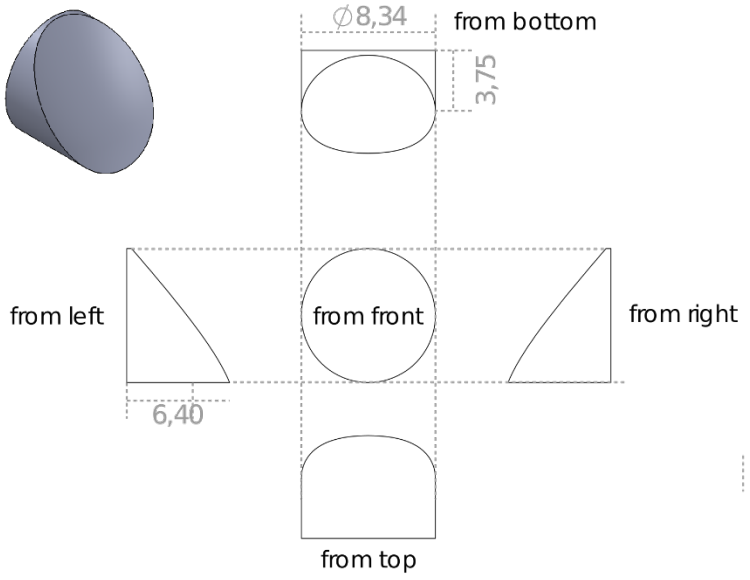

Figure 6: Construction drawing of elliptical mirror eM1. [dimensions in mm]

Because we now wanted to use off-axis elliptical mirrors for directing the beam from the fibre-coupled assemblies to into the cavity, the optical bench had to allow for folding the optical beam. In order to keep the optical bench as small as possible, we decided to fold the beam twice. This approach had two advantages: (1) we should be able to keep the length and the width of the optical bench as short as possible, (2) if we fold the beam twice, we can add optical elements to adjust the various degrees of freedom. This approach allows

to first aligning the cavity and then, independent of that, guiding the optical beam into the cavity.
The outline of the planned setup and the propagation of the optical beams are illustrated in **Figure 24** in the context of WP10 because it is based on a Mathematica model we used to model the influence of temperature changes on the propagation of optical beams in our setup. To describe the beam propagation, let us assume the beam exists from the fibre tip at the right bottom of **Figure 24**. The fibre is held in a ferrule that is placed inside a rectangular glass block (a "ferrule holder") for positioning. This ferrule holder in turn is adhesively bonded to a spacer. From there, the light propagates until it hits an elliptical mirror. That mirror is itself bonded to another spacer for positioning. The reflected beam then is reflected again by a flat mirror that we represented as a prism bonded to a rectangular spacer. From there, the beam passes through the spacer of the first cavity mirror. At the exit of the cavity, after the second cavity mirror, the beam is folded in a similar way until it is coupled into a second fibre on the bottom left of the figure.
While these considerations told us how it should be possible, in principle, to position all the optical elements on the bench, we still needed to consider very carefully how we would mount, move and then adhesively bond the various elements. We will summarize these considerations and our conclusions in the following:

a) Aligning the fibres: for positioning the fibres, we intended to follow the successful example of LISA Pathfinder [4,8] as much as possible. In particular, we adopted the idea of bonding the fibre inside a glass ferrule and then to mount that ferrule in another glass spacer. In our case, we needed additional access to at least some of the rotational and translational degrees of freedom in order to gain full control over the beam direction and position. To this end, we devised a modified setup for a fibre-coupled assembly such that the ferrule holder would be adhesively bonded to the side of a spacer to allow for vertical positioning and for tilting in the vertical plane.
b) Aligning the elliptical mirrors: If we can address the required degrees of freedom in the vertical plane by positioning and pointing the fibre, we still need control over the degrees of freedom in the horizontal plane. We planned to do that using the elliptical mirrors. In particular, the goal was: (1) adhesively bond the elliptical mirror approximately at the right height and rotating the mirror correctly such that the plane of incidence would be horizontal. (2) Once that has been achieved, position and direct the spacer holding the elliptical mirror across the surface of the optical bench.
c) Aligning the flat folding mirrors: If we succeed in the first two points above, then we will not need the flat mirror for adjusting the beam path but only for folding it. For that reason, we decided not to bond a mirror to a spacer as in **Figure 24** but instead simply reflection coat an appropriately flat spacer.

The general **overall alignment procedure** then seemed to be straightforward:

1. Position the two spacers for the cavity mirrors parallel to each other and at the correct distance.
2. Adhesively bond the first cavity mirror to the centre of one of these spacers.
3. Position the second cavity mirror with sufficiently high accuracy on the other spacer, potentially check at this point already if we find the cavity mode. When ready, adhesively bond the second mirror.
4. Once we have found the cavity mode, optimize the coupling into it, and then set up a fibre coupler on the opposite end of the cavity to couple the light transmitted through the cavity. Adjust the distance of the fibre coupler to optimize the coupling into the fibre.
5. Fold the transmitted beam with the flat mirror. The position should be chosen such that we can achieve

the required distance from the cavity mirror to the elliptical mirror. Adhesively bond the flat mirror.

6. Position the elliptical mirror such that it is at the correct height and that its plane of incidence is horizontal. Bond the elliptical mirror to its spacer, but do not yet bond the spacer to the bench.
7. Hold the ferrule holder such that it can move in all degrees of freedom except around the beam axis. Position it to optimize the coupling into the fibre. Once this is done, bond the spacer of the elliptical mirror to the optical bench.
8. Holding the ferrule holder fixed, bond the spacer for the ferrule holder against the ferrule holder.
9. Bond the spacer of the ferrule holder to the optical bench.
10. Switch the direction of the light such that light from the bonded fibre coupler is coupled into the cavity mode.
11. Repeat steps 5-9 on the other side of the cavity.

As we mentioned already in preceding sections, and as we will discuss in more detail below, we only were successful in the first three steps of this procedure.

In designing the optical bench, our main concerns were the following:

- The optical bench plus the optical elements on top should fit into our UHV vacuum chamber, and it should be possible to get the assembly into the chamber via the openings for vacuum flanges. We use an MCF800 spherical-octagon chamber from Kimball Physics with 2¾ CF flanges. It allows for relatively wide and thick objects as long as they are less than 160mm long. Longer objects need to fit into 38mm diameter openings leading to the flanges. This is illustrated in **Figure 7**.
- Because our cavity is comparatively long (97mm), and because it should have a high finesse of ~10^5, the expected linewidth of the cavity resonance is very narrow (~15.4 kHz FWHM). This will make it challenging to find the cavity mode by scanning the laser frequency over the large range of one free spectral range (1.5 GHz). We will discuss our considerations regarding vibrational stability below in more detail.
- Due to the narrow linewidth of the cavity, the thermal stability of the cavity setup is, of course, also a major concern. Because of the considerations described in the previous paragraphs that led us to have all the optical components made of the same material (fused silica), and because of our choice of material for the baseplate (SiC), we expect that the thermal stability of the setup will be excellent.
- In addition to concerns about the thermal stability, a major concern was how to attach the optical bench in a way that would be compatible with an operation at room temperature and an operation at cryogenic temperatures. The issue here is that a mechanical support structure would probably have a very different coefficient of thermal expansion. During cool down, that could lead to high thermal stress or even to damages to the optical bench. We will discuss our considerations regarding the mechanical support in more detail below.
- Aligning the optical elements with high accuracy will require the surface of the optical bench to be polished. After talking to the supplier of the SiC baseplate, it turned out that they will polish the surface of the baseplate to an even higher accuracy than we would have required. In particular, the polishing of the SiC baseplate on the top surface will be of optical quality, sufficient for good mirrors.
- SiC has become a commonly used material for stable mirrors in cryogenic environments in ground-

based telescopes as well as in space. Because these SiC elements are manufactured using sintering, it is possible to manufacture very complicated stable but lightweight shapes from SiC by using thin ribs to stabilize the work pieces. For an example, see Ref. [9]. Because this is a common practice with SiC, we decided to follow the same approach in our design of our optical bench.

In order to test the vacuum compatibility of our cavity setup, we intended to mount our test setup inside a ultra-high vacuum (UHV) chamber we acquired during an earlier research project funded by the European Space Agency (ESA). **Figure 7** illustrates our considerations on the size of our optical bench imposed by the dimensions of that vacuum chamber. At the same time, there was a minimum length of the baseplate such that it could support all optical elements of the cavity as well as the optical elements for coupling light into the cavity and out of it as is illustrated in **Figure 24**. Placing the cavity setup in UHV allows characterizing the cavity setup in a UHV environment without the additional optical delay introduced by the presence of air, and it allows characterizing the stability of the cavity in the absence of air currents.

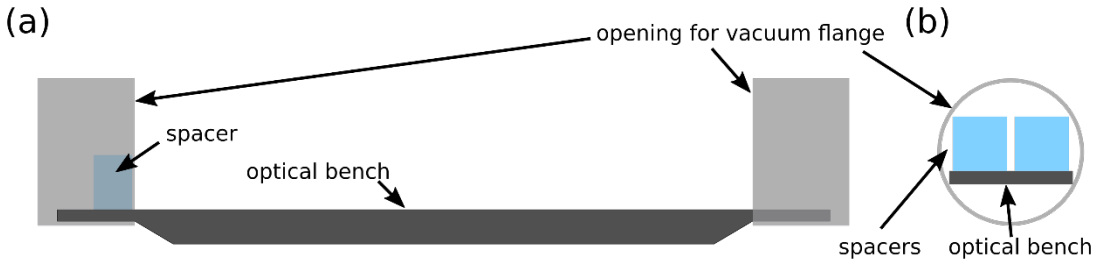

Figure 7: Designing the optical bench to fit into our existing vacuum chamber. Panel (a) shows the size of the flange openings. These are 2¾ CF ports, which defines the diameter of the circular openings. (b) shows a view along the optical bench to illustrate how the size of the spacers limits the maximum thickness of the optical bench.

Because of the length of the cavity setup, it would have to fit into recesses that have a diameter of about 38mm inside the vacuum chamber inside of 2 ¾ inch vacuum flanges. For that reason, the optical bench could only be 3mm thick at both ends. The distance between these two recesses was 160mm. In that space, the optical bench could be thicker to provide additional structural stability. In particular, we decided to have a central part of 140mm length and 9mm thickness that would then taper down to a thickness of 3mm over intervals of 10mm on either end. The 3mm thin parts then were 20mm long on either end, such that the total length of the baseplate was 200mm.

To provide structural stability while, at the same time, reducing the weight of the overall baseplate, the thick part was to have regular pockets of 6mm depth, and each of these pockets was to have dimensions of about

25x25mm^2.

The final design we sent the supplier MERSEN Boostec is shown in **Figure 8**. We are very grateful for the support by Michel Bougoin from MERSEN Boostec for providing valuable input for the design. For example, we originally intended to have cylindrical support arms on the side of the optical bench. Because these would have been too fragile, we replaced them with nearly cubic blocks. In order to provide the possibility for polishing the top surface, the thickness of these mounting blocks needed to be slightly less than the maximum thickness of the baseplate. In order to determine the precise position where to place these mounting blocks, we performed finite-element structural simulations. Michel Bougoin provided us with the necessary SiC material data we needed for that purpose. For the initial alignment of the optical elements at room temperature, we wanted to be able to mount the baseplate using standard posts and post-holders with M4 screws. Therefore, the mounting blocks protruding from the SiC baseplate in **Figure 8** have through holes with 4.8mm diameter. In order to determine the precise position of the mounting blocks extending out from the optical bench, we performed finite element analyses. To this end, we needed to implement a finite-element model of the optical-bench assembly. This was done in WP9. The actual simulations were part of WP10.

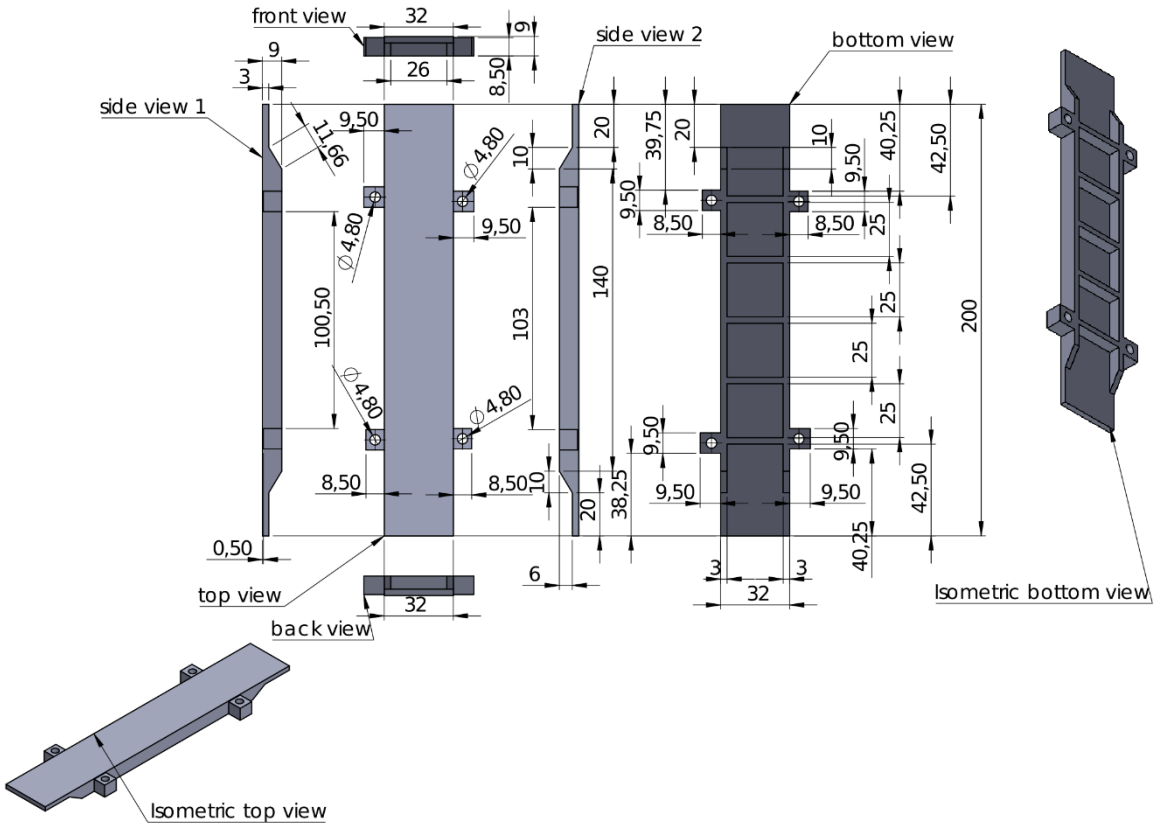

Figure 8: Construction drawing for the SiC baseplate that we sent to the supplier MERSEN Boostec. The supplier further improved the construction drawing by including rounded edges, e.g., in the pockets and on the four support arms in coordination with us. [Dimensions in mm]

In the self-made cryostat of the Aspelmeyer group I was initially meant to use, there was only limited space available. In particular, there would have been no room to mount the optical bench horizontally. The solution we came up with was to mount the optical bench vertically, suspended from optical fibres attached to the mounting blocks of the baseplate. The advantage of this approach was also that it would at the worst lead to

thermal stress in the optical fibres and in the mounting blocks.

For this fibre suspension to work, the two lower mounting blocks needed to protrude from the baseplate slightly more than the upper two mounting blocks such that the fibres holding the lower mounting blocks would not touch the upper mounting blocks. That is why the lower mounting blocks protrude 9.5mm from the optical bench, while the upper mounting blocks protrude only 8.5mm.

With respect to stably mounting the SiC baseplate in a cryostat such that no thermal stress occurs when the temperature of the setup changes from room temperature to cryogenic temperatures, we were considering several options. In particular, the team realizing the Gaia space mission faced a similar challenge because (1) they had to mount two optical benches made of SiC in their payload, and they had to mount fused-silica optical elements to the optical benches. They solved this challenge by using a clamping mechanism that allows for a different thermal expansion of the optical element compared to the SiC baseplate [10]. **Error! Reference source not found.** illustrates that approach. The figure is from the PhD thesis of M. van Veggel [7]. While this method may be of interest for MAQRO in the future, we decided that using this mounting mechanism would go beyond the scope of the present project. Instead, we decided to suspend our SiC optical bench from optical fibres similar to the way that mirrors are suspended from optical fibres in the LIGO gravitational-wave detector [11].

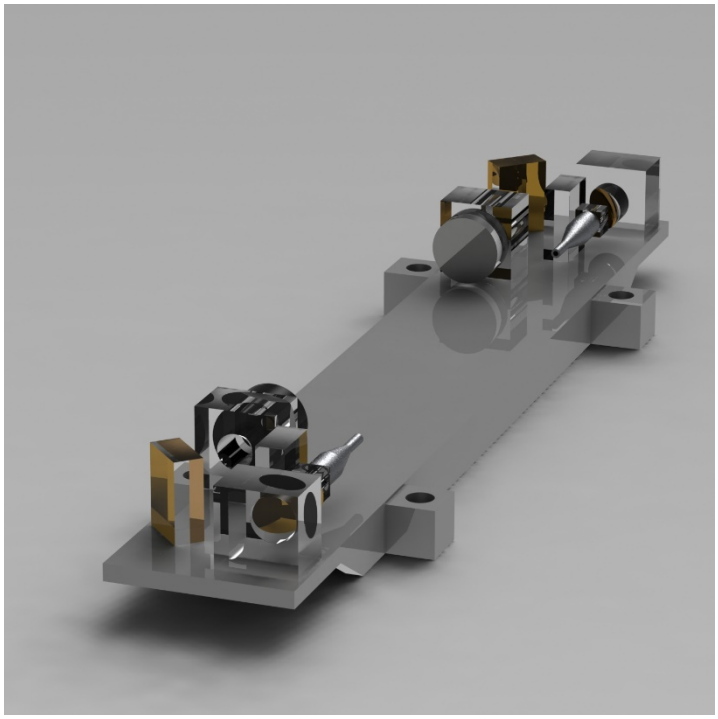

Figure 9: 3D rendering of the fibre-coupled cavity setup on the SiC optical bench. The two silver, cone-shaped structures represent the strain-reliefs for the in and out coupling fibres.

Designing the fibre-mounted assemblies (WP4)

As we mentioned before, the our approach for assembling the optics for coupling light from a fibre into (and out of) the optical setup benefited from earlier work by the group of H. Ward and others in the context of LISA and LISA Pathfinder. Detailed descriptions of many of these efforts can be found in the PhD theses of J.

Bogenstahl [8] and A. Taylor [12].

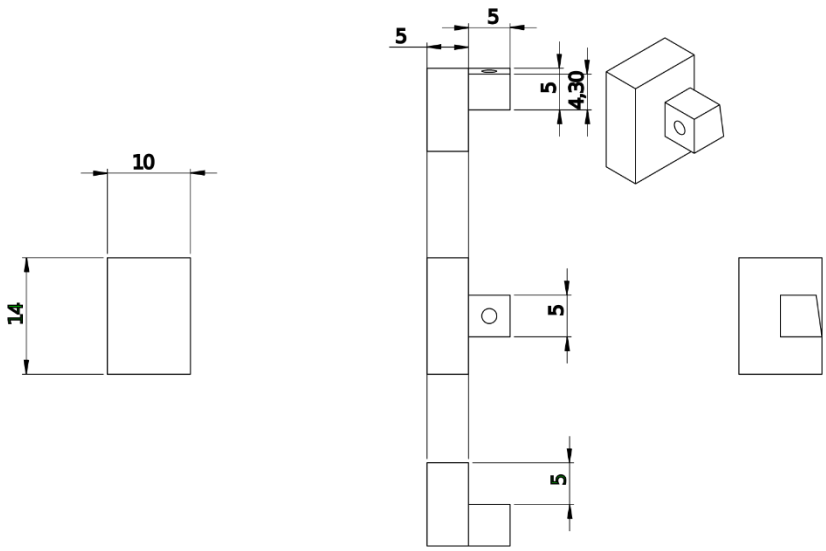

Figure 10: Construction drawing for the fibre-mounted assembly. The figure shows a ferrule holder, which is, in principle a 5x5x5mm^3 cube, but one side is at 98° with the bottom surface. This is meant to reduce back reflections. The centre hole in the ferrule holder has a 1.8mm diameter to hold fitting a fused-silica ferrule for an optical fibre. The ferrule holder is then adhesively bonded to the 10x14mm^2 surface of a spacer with the dimensions 10x14x5mm^3..

In particular, we adopted their approach of bonding the optical fibres into fused-silica ferrules and then bonding these ferrules into fused-silica blocks that can then be used for positioning the fibre tip. Figure 10 shows how the ferrule holder can be moved and along the surface of a fused-silica spacer. This allows an alignment along the vertical direction, and fine alignment of the position of the fibre tip along the direction of the optical beam. One surface of the ferrule holder has an angle of 98° instead of 90° relative to the bottom surface in order to reduce back reflections. In particular, once a fibre inside a fibre ferrule has been adhesively bonded inside the ferrule holder, fibre-polishing sheets can be used to polish the ferrule and the fibre simultaneously to achieve a uniform, optically flat surface of the fibre, the ferrule and the ferrule holder. For this polishing step, we designed and constructed an angled steel disk in which we could mount the ferrule holder containing a ferrule and a fibre. The construction drawing of this polishing disk can be seen in **Figure 11**.

For the polishing disk but also for many other parts we needed for this project, we are very thankful to Roland Blach from the mechanical workshop of the IQOQI Vienna. He worked with incredible precision and speed, and he gave valuable input to our construction drawings. For some parts, it proved very useful that we had a 3D printer in the IQOQI-Vienna workshop. An example is the mirror mount we designed for mounting and

positioning the elliptical mirrors according to the construction drawings in **Figure 12**.

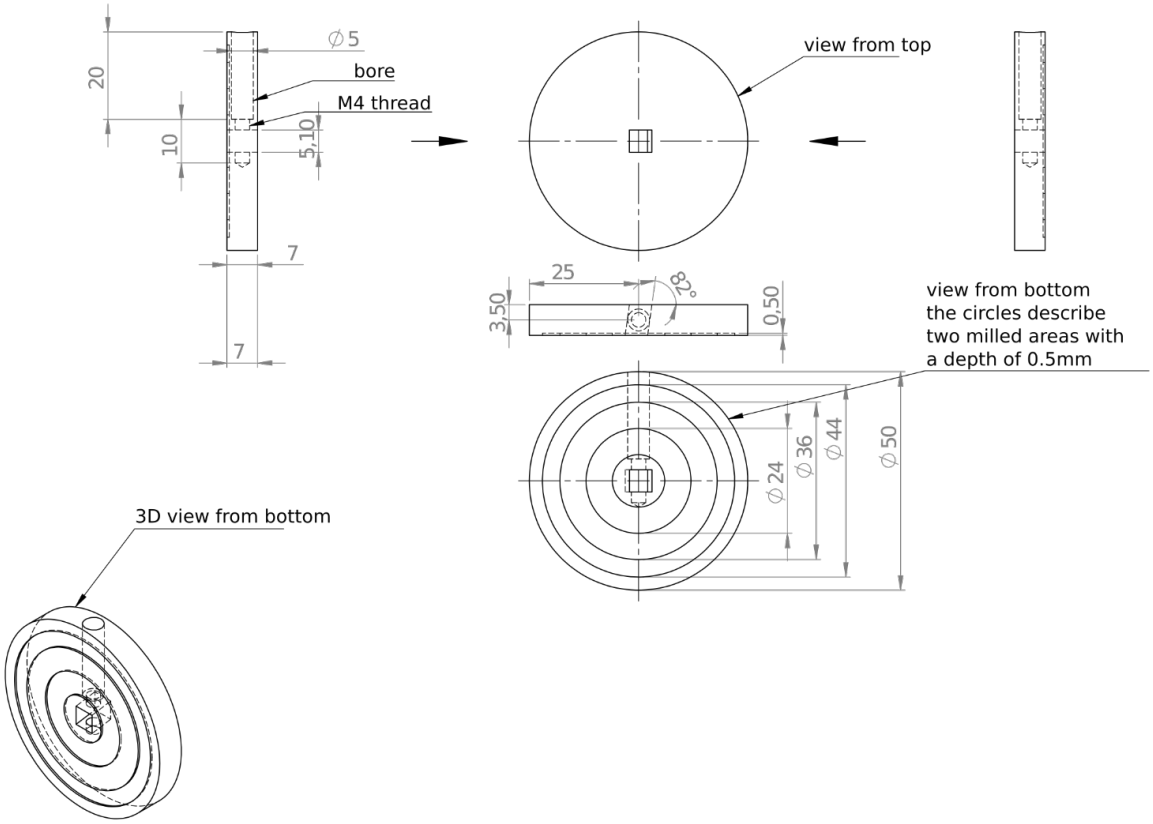

Figure 11: Construction drawing for a steel polishing disk to polish fibre ferrules already containing an adhesively bonded ferrule, which itself contains an adhesively bonded optical fibre. [Dimensions in mm]

Cryogenic tests of adhesives (WP6, WP8)

In total, we acquired four adhesives that could potentially fulfil the requirements we have for adhesive bonding. These requirements were:

- Very low outgassing
- Operates over a wide temperature range from cryogenic temperatures to elevated temperatures more than 100°C.
- Survives repeated thermal cycling.
- Strong adhesive bonds to survive rocket launch while maintaining high-precision optical alignment.
- We need one adhesive with high viscosity for well-defined bonding spots and a low viscosity adhesive for bonding the fibre-mounted assemblies.

We knew from our earlier FFG project MAQROsteps and from our partners ADS and ZARM Technik AG that the adhesives Hysol 9313 and Hysol 9361 from Loctite are space-proof, but the Hysol 9313 adhesive had not been tested at cryogenic temperatures before. On the other hand, the adhesive Hysol 9361 has proved difficult to acquire in Europe already since the MAQROsteps project. Back then, we ended up using Hysol 9313 even

for adhesive bonds where the Hysol 9361 would have been much more suitable.

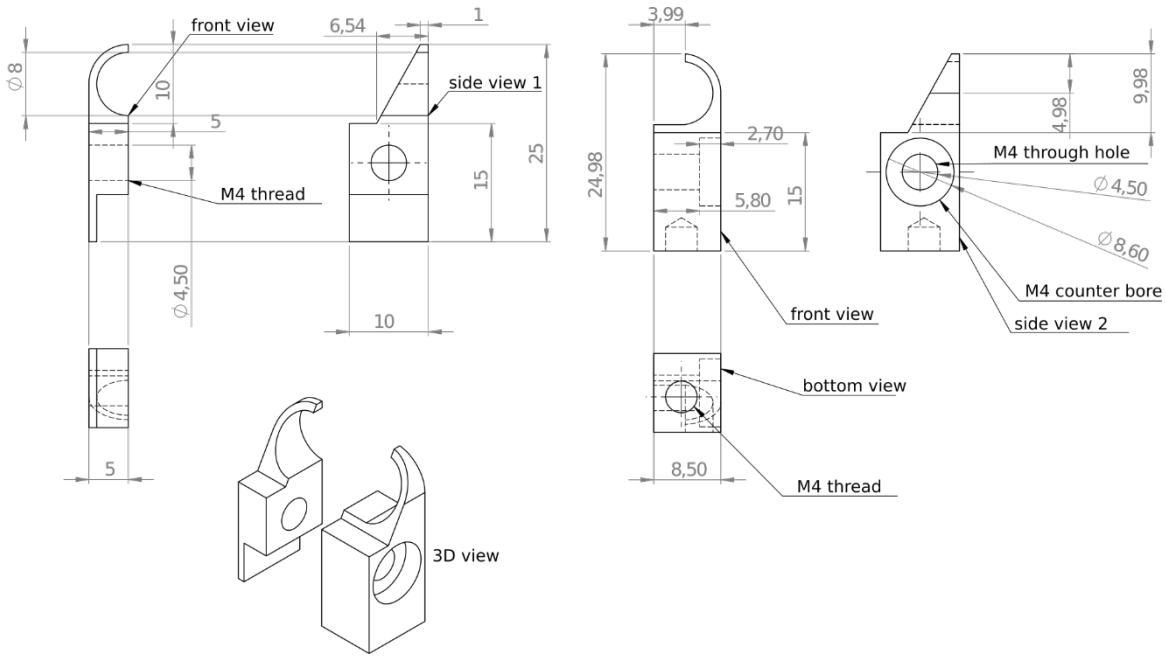

Figure 12: Construction drawings for the two parts of a holder for the two elliptical mirrors. For mounting a mirror, it is clamped between these two parts using the M4 thread and counter bore. Then it is mounted on a post using the M4 thread at the bottom of the piece. [Dimensions in mm]

Because of these reasons, we intended to find potential alternatives to both of these adhesives. After some online research, we found two candidate adhesives from the US-based company Masterbond Inc. Both of these adhesives were certified by NASA to work in a space environment and to fulfil the requirements we listed above. Because it turned out that ZARM Technik AG would be able to supply us with both of the Hysol adhesives, we were in the position to test all four adhesives in order to choose the best-suited ones. In order to test the suitability of the adhesives for our purposes, we wanted to test them at cryogenic temperatures. We will describe these steps in the context of WP8.

Bonding the cavity assembly (WP6)

Once the cryogenic tests of the adhesives and the test assemblies were successfully completed, and after we had decided which adhesives to use, we continued with setting up an alignment setup for the optical components on the optical bench. In a first step, we placed the spacers for the cavity mirrors on the optical bench. To this end, we followed the following steps:

1) We mounted the optical bench on a fixed aluminium mount base aligned along the holes in our optical table. The precision of that alignment was the precision of how well we could visually align the optical bench along the drilled holes in the optical table surface. We asked Roland Blach at the IQOQI-Vienna workshop to make an aluminium part with a thin hole to act as an iris at a specific height and distance from the edge of the SiC bench. By moving this aluminium part along a long edge of the SiC bench, we could make sure that the alignment beam was parallel to the edge of the SiC bench and that the beam was in the position where the cavity mode was meant to be.
2) We positioned the first spacer on the SiC bench by positioning the spacer relative to the edges of the

SiC bench by using aluminium spacers we had constructed by Roland Blach in the IQOQI-Vienna workshop. However, because the accuracy of this approach seemed insufficient, we ended up positioning the spacers using translation stages to push the spacers away from the edge of the SiC bench to the desired position.

3) We set up a 532nm alignment beam emitted from a single-mode fibre. The light was coupled into the fibre on a separate table using our Coherent Verdi V10. By setting up the alignment beam to propagate along the holes in our optical table, we had an additional reference for the alignment of our optical elements relative to the optical table. We illustrate the alignment set-up in **Figure 13**.

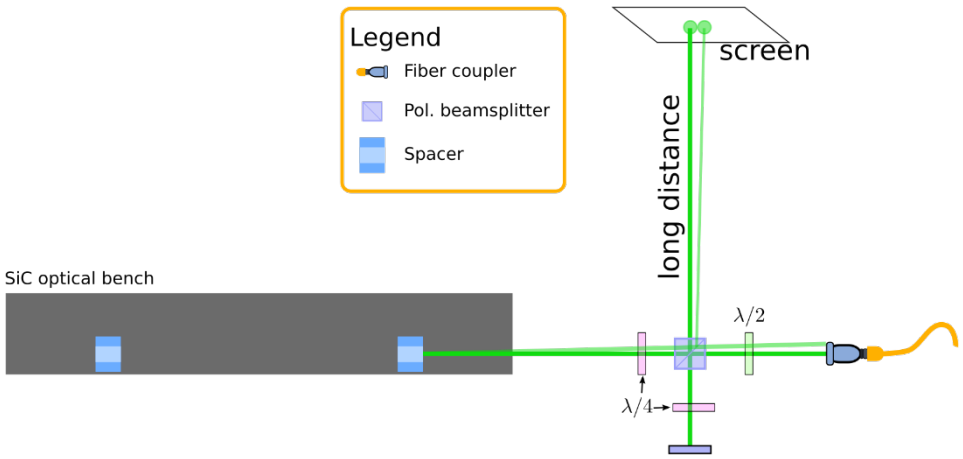

Figure 13: Optical alignment setup to minimize misalignment by monitoring the displacement of back reflections from a reference beam over a long distance. This approach was used to align the fused-silica spacers for the cavity mirrors. We only illustrate the back reflection from the first spacer, but the alignment of the second spacer can be done using the same setup.

As mentioned above, we used a translation stage to move the spacer for the cavity mirror M2 (radius of curvature 30mm) to the correct distance from one of the short edges of the SiC baseplate (35.4mm). Because our translation stage had a maximum travel of 25mm, we placed two spare spacers with a thickness of 10mm each between the aluminium arm attached to the translation stage and the spacer we wanted to position. At the same time, the distance of 1mm from the long edge of the SiC bench was ensured using an aluminium spacer made for us by Roland Blach. Once the spacer was at the correct position, we clamped it down using a micrometer screw. We illustrate this process with the picture in **Figure 14**.

We then applied Hysol 9361 in small spots to the four corners of the spacer to bond it to the SiC bench. During this process and during the time the adhesive took to cure, we monitored the position of the back reflection off the spacer with respect to the reference beam using the alignment setup in **Figure 13**. We then bonded the spacer for the M1 cavity mirror (75mm radius of curvature) in exactly the same way, after also making sure that the distance between the two spacers was correct (109.25mm). We monitored the back reflections for some time after applying the spots of adhesive, and then we let the adhesive cure overnight. During that time, unfortunately, it seems that the curing of the adhesive led to a minute movement of the spacer of M1. Because it was only a small misalignment, we were confident that we could compensate it by correctly positioning M1 itself with respect to the alignment beam and not with respect to the M1 spacer.

The next step was to position and bond the first cavity mirror (M1). To this end, we placed a flat mirror between the two spacers for M1 and M2 at an angle of 45° with respect to the incoming alignment beam. This beam

was then guided on a CCD camera, which we used to determine and monitor the centre of the beam.

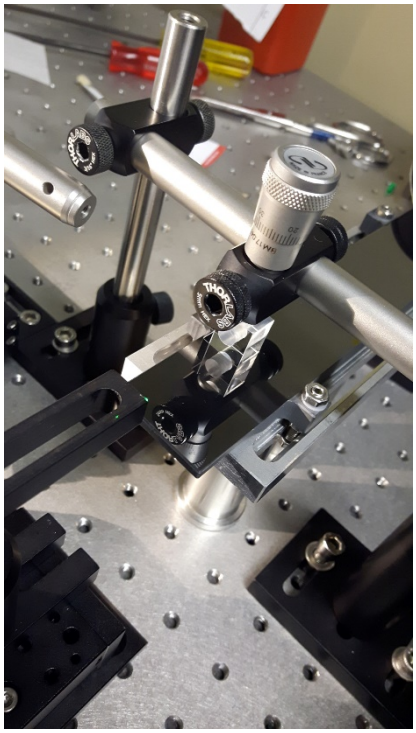

Figure 14: We used a micrometer screw to push clamp the correctly positioned spacer for the M1 cavity mirror on top of the SiC bench. The SiC bench itself is mounted on a custom-made aluminum mounting adapter and 1 inch pedestal posts.

The goal was the following: as soon as we place M1 into the beam, the curved surface of the mirror will focus the green beam. If this focus lies on the same axis as the original alignment beam, then we know that the position of M1 is correct. By monitoring the position of the focused transmitted beam and, at the same time, the back reflection from the flat side of M1, it was possible to position M1 very accurately. We also monitored the transmitted and the reflected beam for some time after adhesively bonding M1 to ensure it would not move with respect to the reference beam.

After successfully bonding the two mirror spacers and the M1 cavity mirror in early 2019, the next step was to position and bond the second cavity mirror, M2. It quickly became apparent that this would be a significantly more difficult task. Because M1 was now an integral part of the bonded setup, it was more difficult to access the M2 mirror with optical alignment beams. We performed a series of attempts to ensure the correct alignment of M2. For this purpose, we used a steadily evolving and improving alignment setup. For the sake of brevity, we will focus on the final setup we used to align M2 and finally bond it. **Figure 16** illustrates this setup.

The central idea here was that we could look at the back-reflections from the cavity setup from M1 or from M2 over long distances of around five metres on each side. By choosing to connect the single-mode fibre with the 532nm light to either C1 or C2, we can choose whether to send the light into the cavity via M1 or via M2, respectively. By putting in a dichroic mirror, we also had the option of feeding 1064nm light into the cavity via coupler C3 and look at back-reflections of 1064nm light or 532nm light using the C4 coupler. We used the pairs of lenses F4 and F4 as well as F6 and F7 to collimate the beam because the distances were large enough for significant beam broadening to occur. This broadening originally led to noticeable clipping of the

beam at the holes of the spacers for M1 and M2. The tricky parts in the alignment were:

- Getting a good reference beam of 532nm light with respect to the already bonded cavity mirror M1 that would travel along the intended cavity mode.
- Making sure that the 1064nm couplers were reasonably well aligned with the green alignment beam.

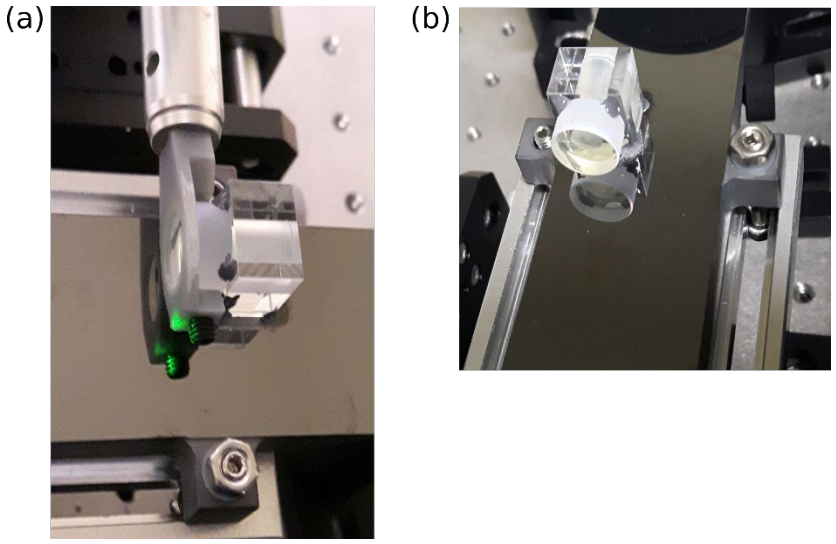

Figure 15: Pictures of the bonding process for the M1 cavity mirror. We used a 3D-printed mirror mount in combination with a tip-tilt platform and an xyz translation stage to position M1 along the surface of M1 while monitoring the back reflection and the transmitted beam.

Until June 2020, we used the following procedure to align the green beam without the PBS and the quarter-wave plate in place for the 1064nm light:

1. Align the light from C1 (without F1 in place) such that the back reflection from the flat side of M1 was overlapping the incoming beam. We ensured that by using several irises in the beam as indicated in Figure 16. Ensure that the broader back reflection from the curved side of M1 is centred around the back reflection from the flat side.
2. Ensure the beam after passing M2 (without F2 in place) was centred on irises between M2 and C2.
3. Optimally couple the light into C2.
4. Send light from C2 instead and repeat the procedure to couple back into C1.
5. Do this iteratively to ensure optimal coupling between C1 and C2 while, at the same time, making sure that the back reflections off M1 are properly aligned.

After aligning the couplers C1 and C2 with the mirror M1 in this way, we put in F1 such that the light would still travel along the same line between C1 and C2. We then put in M2 while looking at the light coming from C1 in order to fix the transverse position of M1. In order to fix the tip/tilt angles of M2, we aimed to centre the back reflections off the flat side of M2 on the irises between M2 and C2.

Because this did not work as precisely as we had hoped, and because the switching of the fibre-connections led to damages of the fibres because of the comparatively high intensities involved, we adapted the alignment procedure in mid-2020. In particular, we decided to keep the light coming from C2 at all times without additional

switching. The irises between M1 and C1 were still in place, and we could use them to align the beam coming from C2 to couple it into C1 (without F1 and F2 in place). We then put in M2 and attempted to align its position as well as its tip and tilt by looking at the back reflections from the flat and the curved side of M2. This was trickier than in the case of M1 because the radius of curvature was significantly smaller for M2. Therefore, the back reflection from the curved side diverged very rapidly. We combined these attempts with making sure that the light from C2 transmitted through M2 was centred on the iris after M1. At the same time, we replaced the low-pass filter between M2 and the webcam with a neutral-density filter to look at the back reflection off M2 on the webcam.

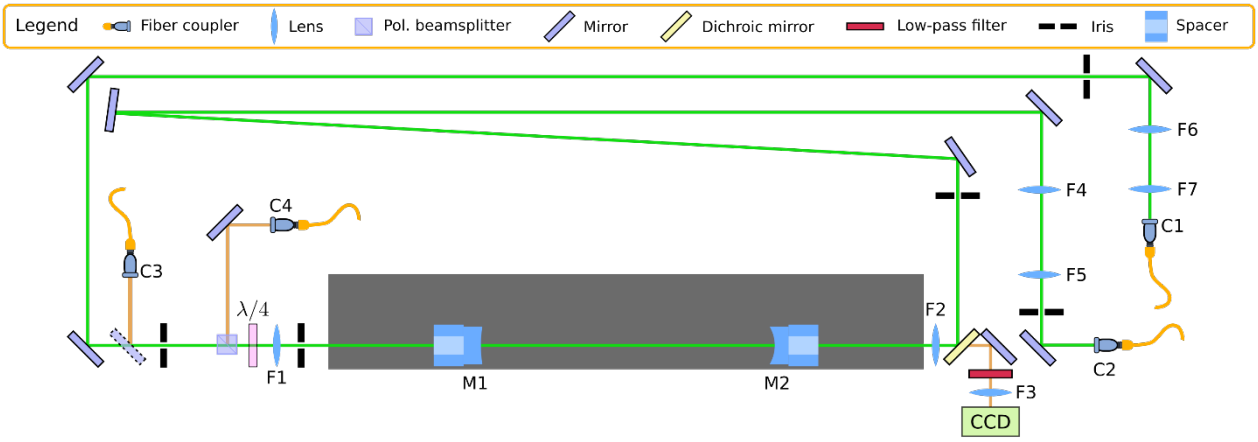

Figure 16: The final setup used for aligning and bonding the M2 cavity mirror. The distances between the mirrors are not to scale compared to the optical bench. The overall green-beam path length is around 10m.

Because we were not yet satisfied that these measures would be accurate enough to define the position of M2, we attempted to align C4 such that we could see cavity modes on the webcam when we performed a regular fast scan of the laser frequency. To check for cavity modes, of course, we used the low-pass filter and not the neutral-density filter in front of the webcam. Because of the narrow linewidth expected for our cavity (around 15 kHz FWHM), we needed to use a comparatively high amount of 1064nm power coming from C4 to actually see cavity modes. The power used was between 60 mW and 100 mW.

By combining all of these measures, we finally were confident enough in early August 2020 to adhesively bond M2. During the bonding process, we monitored the position of the back reflection off M2 on the webcam as well as on the iris closest to C2. We applied the adhesive in the morning such that we had many hours during which the adhesives could begin to cure while we were monitoring the back reflections of alignment beam. We then let the adhesive cure further over night without monitoring the process, but the back reflections were still unchanged on the next day. For that reason, we were reasonably certain that the bonding process completed without any noticeable misalignment.

Characterizing the cavity (WP7)

After we had successfully bonded M2, we spent August and September 2020 on trying to improve the coupling of the 1064nm light from C4 into the cavity. For this purpose, we first aligned C3 and C4 with respect to the green beam coming from C2. Then we attempted to get the back reflection of the 1064nm light off M1 back

into C3 and C4. At the same time, we tried to optimize the speed of the scan of the laser frequency. Unfortunately, we were not successful in significantly improving the coupling of 1064nm light into the cavity before the end of the present project.

The central question now is whether we could not find a good cavity mode because something went wrong in the bonding process, or whether C3 and C4 are simply not sufficiently well aligned, or whether we are still scanning too quickly across the cavity resonance. Another possibility, of course, is that the 1064nm power used is actually too high, such that the intracavity intensity quickly leads to significant heating, driving the cavity out of resonance again. The PI of the project intends to find conclusive answers to these questions and to find the cavity mode if possible. If we are successful, we will be able to set up and adhesively bond the missing parts of the fibre-coupled assembly.

Cryogenic tests and characterization (WP8)

As we mentioned in the context of WP4, we had four candidate adhesives for implementing our prototype. Not all of these adhesives were qualified for being used in a space environment, and our partners from ZARM only had experience with two of these adhesives. For that reason, we wanted to test how well these adhesives would be suited for bonding optical assemblies, and how they would react to to cryogenic temperatures. For that purpose, we decided to bond several test assemblies, and to cool them down to cryogenic temperatures to see whether they would survive the cooling and heating process, and whether the relative alignment of components would change. At the same time, this was an excellent opportunity to test and train how best to realize the different adhesive bonds. For that purpose, Thilo Schuldt from ZARM Technik AG visited with Rainer Kaltenbaek for several days in December 2018. T. Schuldt has worked at ZARM Technik AG and in collaboration with ADS for many years, and he has ample experience in using adhesives for space-proof bonding.

For that purpose, we wanted to implement the following assemblies:

a) A fibre-mounted assembly – i.e., a fibre inside a ferrule, inside a ferrule holder.
b) Two fused-silica spacers on a SiC test plate to test changes in the relative alignment and the bonding between fused silica and a polished SiC surface.

Test (a) is designed for comparing the two low-viscosity adhesives Hysol 9313 and Masterbond EP29LPSP, while test (b) aims at testing the high-viscosity adhesives Hysol 9361 and Masterbond EP21TCHT-1.

For test (b), we ordered two 25x25x3.2mm^3 SiC test pieces from MERSEN Boostec with the top surface polished according to the same specifications as the top surface of the optical bench (lambda@633 nm, S/D40-20), and we used spare fused-silica pieces from our Lens-Optics order to bond them to the SiC

surfaces. **Figure 17** shows the two test assemblies to test the two high-viscosity adhesives.

While bonding the test assemblies, we noted that it was significantly simpler to apply the Hysol 9361 adhesive

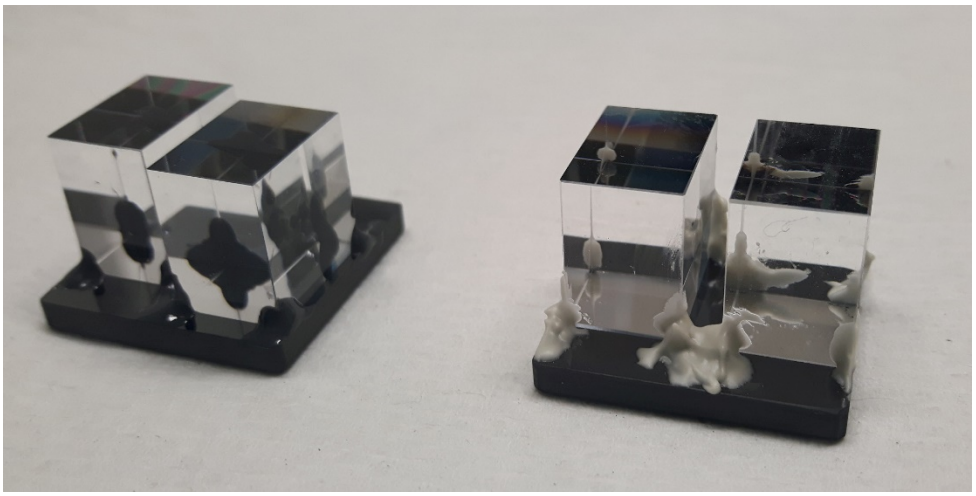

Figure 17: Test assemblies to test the two high-viscosity adhesives Hysol 9361 (left) and Masterbond EP21TCHT-1 (right). The fused-silica pieces are 14x14x10mm^3 solid spacers.

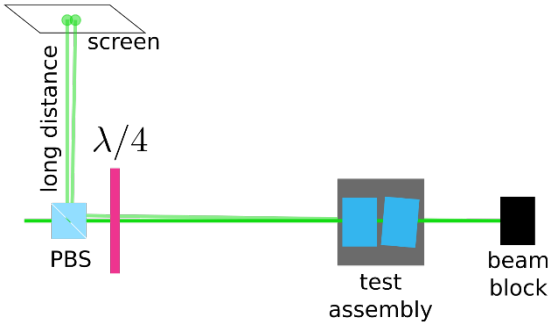

Figure 18: Optical setup to test for misalignments of the test assemblies after placing them in the cryostat and cooling them to cryogenic temperatures. PBS: polarizing beam splitter.

in well-defined spots. The adhesive from Masterbond formed very asymmetric spots and was difficult to detach from the tools we used to apply the adhesive. In addition, the adhesive had an unfortunate tendency to stick to the nearby fused-silica surfaces. In terms of handling, it was already clear at this point that the Hysol 9361 would be the preferred choice – in particular when bonding optical elements with critical surfaces like the cavity mirrors. Getting adhesive stuck to the high-reflectivity surfaces of the cavity mirrors is a no-go. Despite of that,

we still wanted to continue and test the assemblies in the cryostat.

All four adhesives were two-component epoxies. In order to mix the two components of the adhesives, we used E-2130 Petri dishes. These are made of glass, have a diameter of 40mm and a height of 12mm. We used a double spatula to mix the two components of the epoxies in the Petri dish. We kept all the Petri dishes for later reference. For all the adhesives used, the two components had to be mixed according to specific mass ratios. To this end, we used a scale with mg resolution available at the sample preparation room of the University of Vienna.

To test whether the cooling of the test assemblies would affect the relative alignment of the bonded components, we used a 532nm alignment beam from a Coherent Verdi V10. In particular, we sent the alignment beam through a combination of a polarizing beam splitter (PBS) and a quarter-wave plate to separate the back reflections from the incoming beam. Because the light was reflected from two spacers, there were four interfaces between air and fused silica. That resulted in two back reflections from each of the two spacers. After propagating the back-reflected beams over a distance of about five metres, we marked the positions of the back-reflected beams on a sheet of paper for later reference.

Because we wanted to be able to remove the test assemblies from the alignment beam to place them into the cryostat and then see whether the fused-silica blocks moved relative to each other. To this end, we positioned the SiC plate of each of the test setups against two aluminium blocks for later reference (see **Figure 19**).

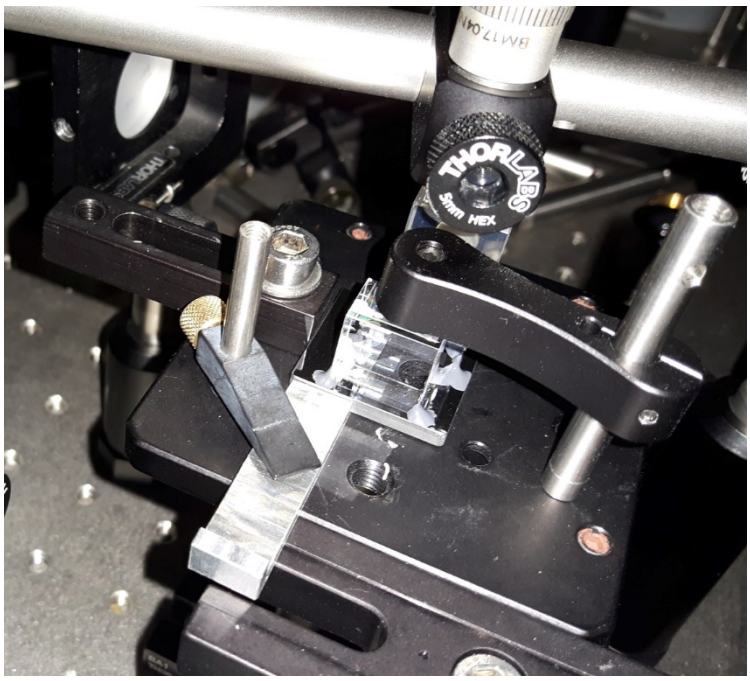

Figure 19: We used two aluminum pieces to define the position of the test assembly to allow removing the test assembly and then placing it back at the same position again later.

The fibre assembly had to be assembled in two steps. First, the SMF-28-J9 glass fibres (125µm cladding around the 8.2µm core) had to be adhesively bonded into fused-silica ferrules. These had an outer diameter of 1.8mm +/- 20µm. The inner hole for the fibre had a diameter of 127 +3/-1µm. To this end, we followed the

following steps:

I. We removed part of the outer protective coat from the fibre to expose the naked fibre.
II. Move a glass ferrule onto the exposed fibre.
III. Put a bit of adhesive close to where the protective coat ends and the exposed cladding begins.
IV. Move the ferrule over the region with adhesive against the position where the coat begins.

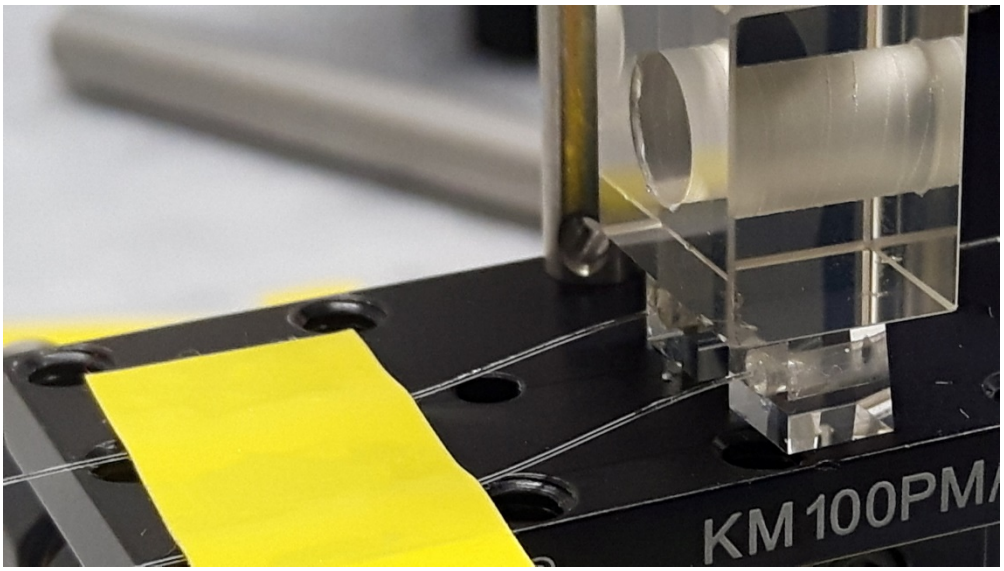

Figure 20: Curing the adhesives in two fibre-mounted assemblies at room temperature. Both assemblies are clamped to a prism table. A spare Zerodur spacer for cavity mirrors from the MAQROsteps project is used to clamp both assemblies simultaneously. The fibres are secured using a yellow sticky tape acting as a stress relief during the curing process.

Typically, we aimed for the fibre to stick out several mm from the end of the ferrule. After the procedure described above, we had to let the adhesive cure. **Figure 20** shows a photo of how we cured two fibre-mounted assemblies at room temperature. In the case of Hysol 9313, this can be done at room temperature, but it can be accelerated by using higher temperatures. If one uses the Masterbond EP29LPSP adhesive, it is necessary to first cure the adhesive at room temperature for around 6 hours (see Figure 20). After that, the assembly needs to be cured at 200°F for about 5 hours. To this end, we placed the ferrules with the fibres into a baking oven in the sample preparation room of the University of Vienna.

Once we had bonded several ferrules to optical fibres using this procedure, the next step was to bond the ferrules into the ferrule holders. To this end, we followed the following steps:

1) Move the ferrule (with the fibre) through the hole in the ferrule holder. Place the aluminium block with the small hole the fibre is passing through against the ferrule holder.
2) Put (very little) adhesive on the outside of the ferrule.
3) Pull the ferrule back through the ferrule holder until the flat ends of the ferrule and the ferrule holder are aligned. This can be ensured, e.g., by pulling the ferrule up against a thin Allen wrench placed at

the back end of the ferrule holder against the fibre.

After we finished assembling and curing the fibre-mounted assemblies and the SiC-silica test assemblies, we placed them into the 4K stage of one of the dilution refrigerators of the Aspelmeyer group (see **Figure 21**). We were able to achieve a temperature around 8K in the cryostat. While this was higher than the 4K we expected, it was significantly lower than the 16-20K we aimed for originally. The cooling process from room temperature to 8K took about two days. The warming-up process took around one day. We repeated this cooling and heating procedure a few times. During these tests, the 4K stage was pumped to about 10^{-6} mbar by a combination of a membrane pre-pump, a turbo pump and cryo-pumping. As can be seen in Figure 21, the volume available inside the cryostat was much larger than what we needed for these tests or even for the tests of the full cavity setup.

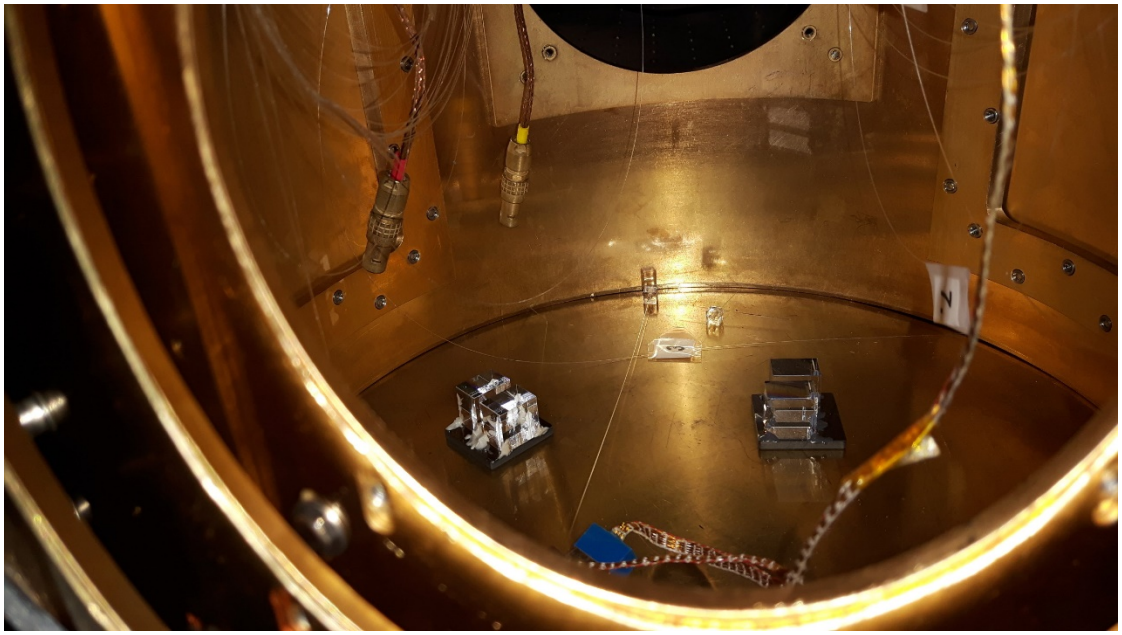

Figure 21: The SiC-Silica test assemblies and the fibre-mounted assemblies inside the dilution fridge. In the front, one can see the three copper shields for the different temperature stages of the fridge. The reader looks into the 4K stage. Several optical fibres are visible that could be used to connect our fibre-coupled cavity setup.

After the test in the cryostat, we placed the SiC-Silica test assemblies into the optical test setup again and tried to re-align the back reflections with the markings we had made earlier on the sheet of paper we mentioned above. This procedure showed that no noticeable misalignment occurred in the test assemblies due to the cooling and re-heating. That means, this part of the test was successful, and both high-viscosity adhesives should be suitable for our purpose of bonding optical setups for applications in a space environment.

On the other hand, we noticed a change in the colour of the Hysol 9313 adhesive in the fibre-mounted assemblies. Given that Hysol 9313 is not specified by the manufacturer to work at cryogenic temperatures, we concluded, that the safest course of action would be to use the Masterbond EP29LPSP adhesive for our fibre-mounted assemblies.

Given that the test was successful for the Hysol 9361 and for the Masterbond EP21TCHT-1 adhesive, we decided to use Hysol 9361 for the cavity setup because the adhesive was much simpler to handle and to apply

in well-defined adhesive spots.

Definition of a finite-element thermal model of the optical bench (WP9)

We followed two approaches to study the thermal behaviour of our optical-bench assembly: (a) we developed a model in Mathematica to calculate changes to the location and the shape of optical elements as well as to calculate the resulting changes to beam paths and beam parameters. (b) We implemented finite-element model in COMSOL Multiphysics in order to study thermal deformations and thermal stress resulting from changes to the temperature of the optical assembly.

In order to implement the finite-element model in COMSOL, we first had to become familiar with the Thermal Simulation module of COMSOL. To this end, we first implemented several very simple simulations consisting only of two separate cubes or of other simple geometric forms. We did so, in order to (a) investigate how to best implement the interface between different elements to simulate the thermal conduction, (b) run simulations with different combinations of materials, (c) compare steady-state and time-dependent simulations, (d) study possible ways how to integrate adhesive bonds in our simulations.

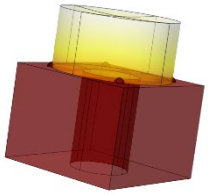

Figure 22: Finite-element simulation of heat transfer from a silica spacer ($14 \times 14 \times 10$ mm^3) with a clearance hole for the optical beam and a spherical mirror. The mirror in this simulation is adhesively bonded to the spacer via four localized positions (the small spherical spots).

In the further course of our investigation, we quickly found that it would be very challenging to perform time-dependent thermal simulations because that required a very precise knowledge of the interfaces and the thermal conduction. In particular, the thermal conductivity across these interfaces will depend on the precise material properties of the adhesives used, on the area covered by the adhesives, the thickness of the adhesive layer, and on the amount of stress in the interfaces because higher thermal stress may actually lead to a stronger thermal contact between the bonded elements. Moreover, a precise modelling of the adhesive bonds would have required 3D modelling. For example, **Figure 22** shows a 3D simulation of the heat transfer from a fused-silica spacer to a fused-silica cavity mirror adhesively bonded to a spacer. In this particular simulation, one can see that there is only very little heat transfer because (a) there is no pressure pushing the mirror against the spacer, (b) we assumed that the adhesive bond has a very low thermal conductivity.

While we expected that the use of localized adhesive bonds would lead to less thermal stress in the bonded components, we expected that this approach may result in unpredictable displacements of the optical elements during cool down because it will be difficult to achieve identical bond strengths for all bonds involved. In discussions, our sub-contractor ZARM Technik AG made us aware that the use of localized spots for bonding would definitely be the best choice when bonding different materials or when bonding highly sensitive

optical elements. If the spots used for bonding are small, then small differences in the volume of these spots should lead only to negligible relative shifts of the bonded optical components. For these reasons, we decided very soon after the two intermediary reports that we would use localized spots of adhesive for bonding sensitive optical components like the cavity mirrors (see **Figure 22**).

Figure 23: To model how our cavity would be affected by temperature changes, we assumed the spacers of the cavity mirrors to be fixed to the optical bench at their center (red dots). The distance between these points changed according to the coefficient of thermal expansion (CTE) of the optical bench material. The distances between the red dots and the respective mirror centers depend on the CTE of the material of the spacers and the cavity mirrors.

In the following, we avoided the complexity of 3D simulations and focused on steady-state thermal simulations using COMSOL and Mathematica. These helped us better understand when and how thermal stress would occur in the optical-bench assembly and how the geometry would be affected by thermal expansion. **Figure 23** shows the sketch of our core cavity assembly to illustrate a simplifying assumption we made in modelling thermal expansion in Mathematica. In particular, we assumed that elements were attached to each other at their geometrical centre of the areas where the elements were attached to each other. In this particular example, the mirrors would be rigidly attached to the spacer, and the spacers are connected to the baseplate at the points indicated.

The most prominent advantage of using a SiC baseplate is that the instantaneous coefficient of thermal expansion and its slope over changes of temperature are very small for SiC at low temperatures. Other advantages of SiC are: (1) the material can be sintered into to very complex shapes, as we will see later when we present the design of our optical bench. (2) its density and heat capacity are low, and (3) its mechanical properties are beneficial at low temperatures. (4) As we can see from **Figure 28**, the rate at which the cavity length changes with temperature is lower for SiC than for fused silica at low operating temperatures. This becomes even more apparent if we plot the change of the free-spectral range of the cavity (see **Figure 30**). For these reasons, we decided to use a SiC baseplate for our setup as well as for the optical bench of MAQRO.

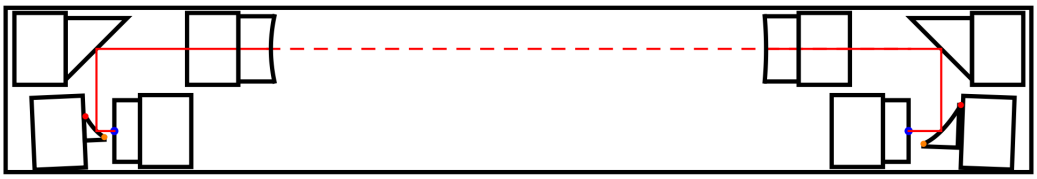

Figure 24: Folded design of the cavity test setup. The sold red line indicates the beam path. The dashed red line indicates the cavity mode. The blue dots represent the fibre tips. The orange and red dots show the edges of the elliptical mirrors. The spacers for the elliptical mirrors are slightly rotated around the vertical axis in order to align the major axes of the ellipsoids with the cavity mode. For this figure, we assumed the baseplate top surface to be 200x32mm². Distances and element dimensions are to scale.

Figure 23 illustrates the basic concept we used to model thermal expansion in Mathematica. Using this approach, we modelled the full optical path of light coupled out of a fibre, into the cavity and then back into a fibre in our prototype setup. We illustrate this model in **Figure 24**. Using this model, we could track the beam path as well as the evolution of the beam waist in the optical setup in order to investigate potential changes if

the temperature of the assembly changes. Using this model, we found that the changes due to thermal expansion of the SiC baseplate should be negligible, and we could conclude that, because all optical elements consist of fused silica, there would be no relevant changes to the propagation direction of the light. Because we use elliptical mirrors for focusing into and out of the cavity, changes to the focal points and the waist sizes will also be negligible.

Simulation of the thermal and the structural behaviour of the optical bench (WP10)

In the context of WP4, we described the considerations behind having “mounting blocks” protruding from the SiC baseplate such that we would be able to mount it on an optical table or to suspend it from optical fibres. To determine the precise position of these mounting blocks, we implemented a full structural model of the baseplate plus the optical elements on top of it. The goal was to find the vibrational eigenfrequencies of the setup and the locations of the nodes of the fundamental vibration mode. We intended to position the mounting blocks at the nodes of the fundamental vibration mode in order to reduce the coupling of vibrations via the mechanical support from the environment to the optical bench.

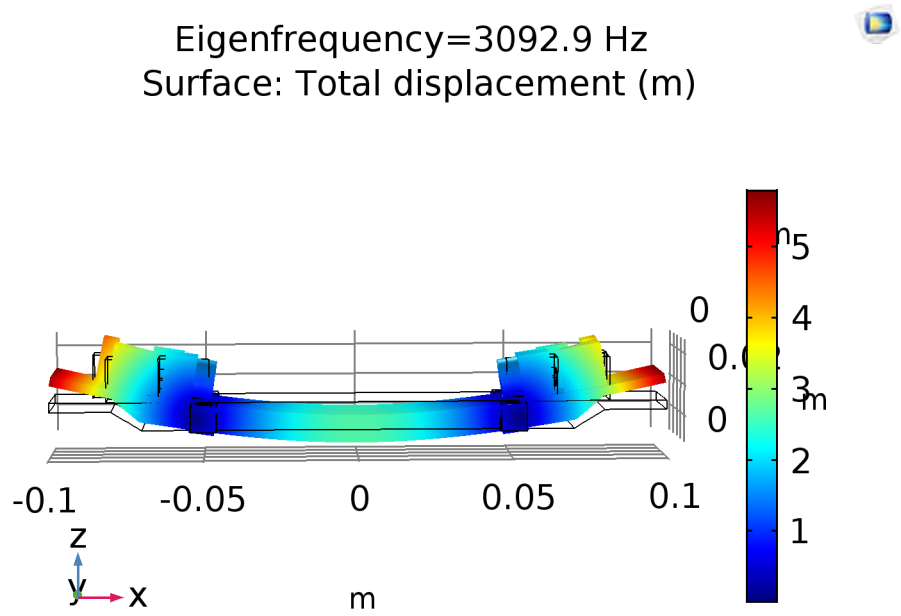

Figure 25: The fundamental vibrational mode when the SiC baseplate does not have structural recess pockets has a higher eigenfrequency than in Figure 13. The relevant information here is the position of the vibration nodes and the eigenfrequency. The values for the total displacement are not representative.

Figure 25 shows the fundamental vibrational mode of the setup on top a SiC baseplate. In this simulation, the eigenfrequency is higher than what we will see in later simulations because this model did not include structural pockets. We included them at a later point to reduce the overall weight of the baseplate. Because it is possible to sinter SiC in nearly arbitrary shapes, it is a common practice to use such structural pockets, for example to reduce the mass budget in space instrumentation. **Figure 26** shows a similar simulation that includes trigonal structural pockets. After discussing with Michel Bougoin from MERSEN Boostec, we followed his suggestion to use rectangular pockets instead of trigonal ones. At this point, we did not redo the finite-element simulations to avoid further delays. That means the positions of the mounting blocks of the actual setup are not exactly at

the optimal positions.

Because there are more optical elements on one side of the optical setup shown in Figure 24, the positions of the vibrational nodes and the positions of the mounting blocks are slightly asymmetric from one side to the other on the optical bench. This can be seen in the construction drawing in Figure 8.

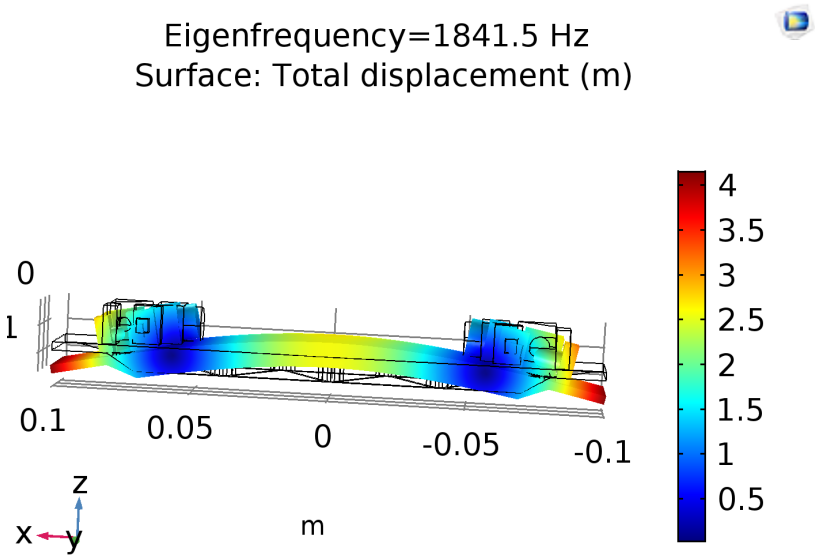

Figure 26: The fundamental vibrational mode of the setup with trigonal pockets to reduce the overall weight of the optical bench.

To perform thermal finite-element modelling using COMSOL, we first did some simple initial simulations where we tried to become familiar with how COMSOL handles the material definitions, the definition of interfaces etc like we mentioned in the context of WP10.

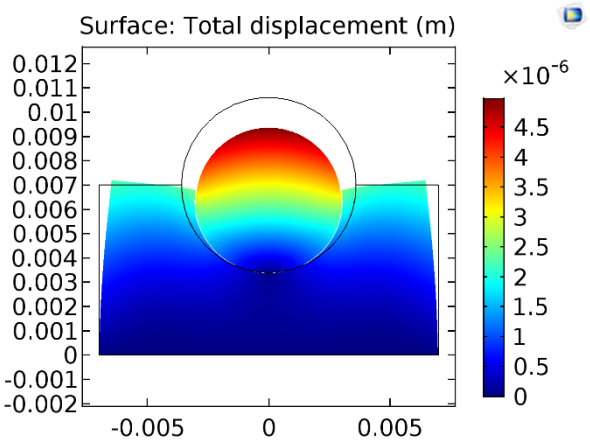

Figure 27: This image illustrates the distortion of a simple optical assembly predicted by a COMSOL finite-element simulation, where a lens made of Pyrex glass is adhesively bonded into a U-groove of a silica substrate. While it is conceivable to compensate the overall displacement, the different coefficients of thermal expansion lead to thermal stress throughout the lens, which would also distort optical modes transmitted through the lens.

For example, the results of a very early simulation we ran is shown in **Figure 27**. Here, we wanted to compare the thermal expansion of different glass substrates when we cool them down to cryogenic temperatures. In this particular simulation, we compared Pyrex and fused silica, because we wanted to use fused silica for the

spacers for optical elements, and Pyrex was a possible material choice for the aspheric lenses we planned to use to couple light from the fibres into the cavity mode. The results of this simple simulation illustrate that significant thermal tension would occur during a cool down from room temperature to cryogenic temperatures. The U-groove design in this simulation was inspired by a U-groove design that was considered for fibre coupling assemblies for LISA Pathfinder [8]. In LISA Pathfinder, the final design consisted only of components of fused silica to avoid potential issues like thermal stress.

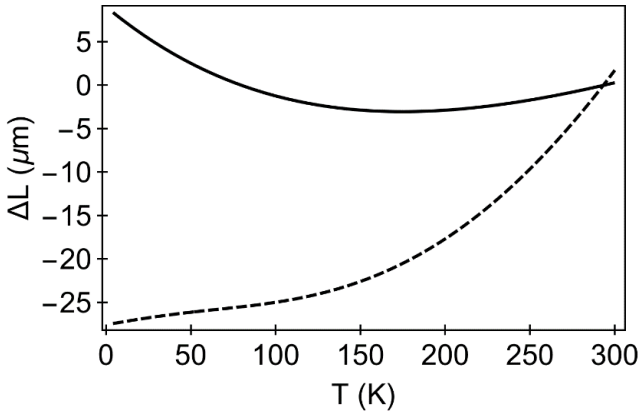

Figure 28: The figure shows the change in the cavity length as a function of the ambient temperature. The solid line is for a fused-silica baseplate (Corning 7980), and the dashed line is for a SiC baseplate.

The models we made in Mathematica to describe the effects of temperature changes and of thermal expansion were very simple. Let us first discuss how we modelled the propagation of light through aspheric lenses. This was central in the early stages of this project when we were still planning to use aspheric lenses to couple into and out of our optical cavity assembly. (a) In the case of describing the beam propagation through aspheric lenses, we took into account changes to the shape of the aspheric lens as well as changes to the refractive index. Changes in the shape as well as the refractive index led to a change and in angles of refraction. Even in cases where the angle of refraction does not change, a change in the refractive index will lead to a change in the optical path length. To model aspheric lenses in Mathematica, we propagated a bundle of rays with a finite aperture through the lens and determined for each ray where it would intersect the optical axis again after the lens, and we calculated the optical path length between a start plane to the intersection point. The goal was that all rays should meet at an intended focal point after having travelled the same optical path length. We found the corresponding lens shape by numerically solving a differential equation. Then we generated data points representing the lens shape, and we fitted an aspheric lens shape according to equ. (1)(1) to that data set. Once we found an optimal shape for an aspheric lens at room temperature, we again analysed the propagation of a bundle of rays through the lens. As we described earlier, we found that the change in refractive index with temperature will lead to significant discrepancies at cryogenic temperatures. For that

reason, we adapted our designs to use elliptical mirrors instead.

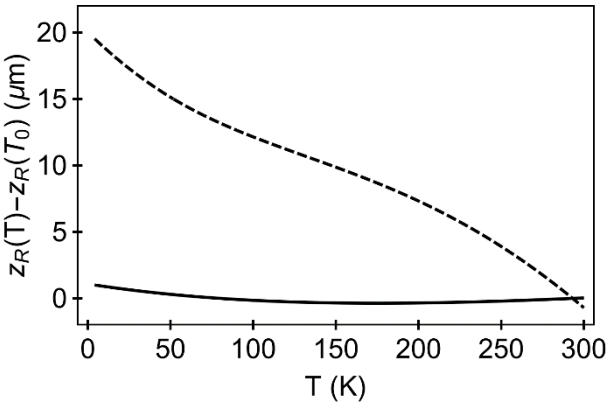

Figure 29: Change of the Rayleigh length as a function of temperature in the case of a fused-silica baseplate (solid line), and in the case of a SiC baseplate (dashed line).

Apart from modelling the aspheric lenses, we also used Mathematica to determine how the choice of different materials for the optical bench and the spacers and optical elements would affect the cavity and the coupling of light into the cavity. In terms of thermal stability, it was clear that Silicon Carbide (SiC) would be the best choice for MAQRO because SiC is ultra-stable against temperature variations at cryogenic temperatures. In addition, we saw in thermal studies in the course of MAQROsteps that the lower heat capacity of SiC is advantageous in the context of MAQRO [13]. Nevertheless, we wanted to analyse what effects choosing an optical bench of SiC would have on the cavity mode and the cavity resonance.

Figure 28 shows that the change in the cavity length as we cool the setup from room temperature to cryogenic temperatures is small in both cases, but fused silica actually shows less change. Similarly, the change of the Rayleigh length of the cavity mode is larger for a SiC baseplate, but it is only a very small change compared to the Rayleigh length, which is about 12mm. We show that in **Figure 29**. For **Figure 28** and **Figure 29**, we made the simplifying assumption that the spacer carrying the cavity mirror is attached to the optical base at a point in the spacer's centre. We illustrated in the context of WP9 in **Figure 23**.

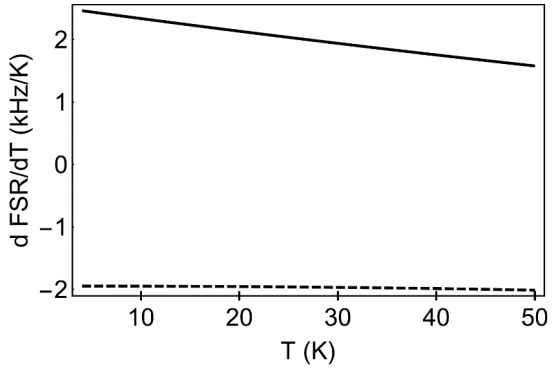

Figure 30: Susceptibility of the cavity resonance to changes of the temperature. The graph shows that the response of the cavity resonance frequency to temperature changes is noticeably more stable for a SiC optical bench (dashed line) than for a fused-silica optical bench (solid line).

2.3 Changes in the further course of the project

Because this is the final report, there are no changes to the "further course" of the present project, but the PI

will continue implementing the fibre-based cavity setup due to its significance to the MAQRO mission proposal. Effectively, the setup we started implementing in this project is a prototype realization of the optical bench of MAQRO. Design decisions we made for this setup were immediately adopted for the proposed payload of MAQRO and for the QPPF study at ESA's concurrent design facility. Due to a misunderstanding of the prototype concept in FFG grants, we failed to declare our prototype as a prototype at the beginning of the project. We remedied that later on. All material and all components bought during the project went directly into the prototype, were adhesively bonded, and cannot be taken apart without significant damage.

Because the design and the acquisition phases of the project took significantly longer than anticipated, it became clear in late 2018 and early 2019 that the remaining steps would take too long to finish the project in March 2019. For that reason, we decided to extend the duration of the project by one year. Due to additional delays because of COVID in 2020, we finally extended the run-time of the project until the end of September 2020.

The project leader has had to reduce his availability to work on the present project since the beginning of 2019 because (a) he was also the PI of a second FFG project (QuantumShield), and (b) because the PI started his own research group at the University of Ljubljana in March 2019. From that point onward, the PI had to commute between Vienna and Ljubljana to continue supervising the running FFG projects ULE-Cavity-Access and QuantumShield.

3. Project team and cooperation

There have been no changes in the cooperation with ZARM Technik AG, and we concluded this cooperation successfully. There help was invaluable in acquiring the necessary adhesives and in gaining the required experience in adhesively bonding optical setups.

The cooperation with ADS initially worked as planned, but after Ulrich Johann went into retirement and Michael Chwalla was reassigned internally by ADS to work on other projects, the responsible project manager at ADS became Domenico Gerardi, and the frequency and the level of cooperation reduced significantly. While the cooperation continued, ADS never signed a contract for the cooperation, and we agreed at some point that they would not send us an invoice. This was communicated to the FFG via ecall. At that point, it had already become clear that we would use a cryostat at the University of Vienna and would not have to rely on a cryostat at the ADS premises. In addition, Thilo Schuldt from ZARM Technik AG regularly works at the ADS premises, which helped with continuing the contact to ADS and our access to their expertise in bonding technologies. Because of that, these changes did not have any significant effect on the project apart from the positive financial aspect that we could use the money initially reserved for ADS for other purposes in the present project.

While the project team in Vienna remained the same throughout the last reporting period, the PI of the project had to reduce his work on the present project due to other obligations. This has been described in section 2.3. Because the PI focused his time on the remaining work packages, the effects of his reduced availability could be held to a minimum, and because this change only occurred during the last year of the present project, the effects were limited. In future projects, however, the PI will aim to include students or postdoctoral researchers

in order to keep up with the allotted workload.

4. Final Report only: Dissemination and exploitation

The PI presented the work in this project during many of this presentations at international workshops and conferences. The design for the fibre-coupled cavity assembly was adopted for the MAQRO mission proposal and, in particular, for the design of the payload studied in the QPPF study by ESA at their Concurrent Design Facility. The final report of the QPPF study is available here:
https://sci.esa.int/web/future-missions-department/-/61074-cdf-study-report-qppf
The publication of several papers related to the MAQRO mission proposal is currently in process, and this project will be mentioned in the acknowledgements. Because this project had a significant impact on the payload design of MAQRO and QPPF, it will continue being acknowledged in future papers concerning the fibre-coupled cavity setups and the adhesive bonding of the optical setup in MAQRO.
The PI strongly intends to continue characterizing the cavity setup and adding the missing optical components to complete the fibre-coupled setup. If successful, the results be published in a peer-reviewed journal. Even if we are not successful, we will aim to publish a paper based on this final report to describe the bonding procedure we developed for fibre-coupled optical cavities.
If we are successful in implementing the fibre-coupled cavity setup, we intend to use it in future proof-of-principle optomechanical experiments, and potentially in free-fall experiments and in optomechanical experiments at cryogenic temperatures.

5. Explanatory notes on cost

As we mentioned earlier, a few changes led to a re-allocation of costs in the present project:

- ADS did not sign a contract for the cooperation in this project, because the extent of the cooperation was less than originally planned, and because ADS subsequently did not charge us for the cooperation. The funds originally allocated for this cooperation were re-allocated to other expenses in the course of the project. We discussed these changes with the FFG via ecall.
- The PI has not employed for 100% since the beginning of 2019 because 10% of his time were allocated for the FFG project QuantumShield. Since March 2019, the PI was only employed for 10% on the present project because of his new position in Ljubljana.

We have not mentioned so far that, for a short time, the PI trained the master student Yao Zhou on the optical setup used for aligning the cavity mirrors. In particular, the student learned how to read out images from a webcam for monitoring the position of the alignment beam, to clean optics, to use optical beams to align optical components, and to scan the frequency of our Coherent Mephisto to search for cavity modes. This was a good opportunity for the master student to gain some experience in working in a quantum-optics laboratory, and the costs for his marginal employment were small compared to the personnel costs for the PI.

Another important change was that the setup built was declared as a prototype. As we mentioned earlier, we should have done that right in the beginning because our work in this project is a perfect example of a prototype, but we failed to consider that at the start of the project. While this did not lead to any additional

costs, it changed the depreciation times for some of the parts of the setup because everything was part of the prototype. Since we only noticed very late that what we were building should be declared as a prototype, this did not encompass acquisitions we had made earlier, when the PI and the project still were at the University of Vienna.

Asset utilization, acquisition cost

- COMSOL Multiphysics Network License - € 11,495.00
  These are licenses for the COMSOL finite-element simulation software and for additional modules of that software. In particular, these are:
  - COMSOL Structural-Mechanics Module
    A module to perform finite-element simulations of vibrations, stress etc. We used it to analyse the vibrational eigenfrequencies of our optical setup in order to determine where to position the mounting blocks on the SiC baseplate.
  - COMSOL Heat-Transfer Module
    We used it in finite-element simulations to see how temperature changes affect optical assemblies in our setup.
  - COMSOL Material Library
    These are additional material parameters we used to simulate our setup. For example, this contained the definitions for the fused-silica components we used.

Costs of Materials

- Prototype Cavity Access - € 24,503.18
  This contains all material and components what we used to build our prototype setup starting in 2019 because we had not realized earlier, that our work perfectly fits the definition of a prototype. The prototype contains some of the crucial components of our setup like the SiC baseplate and the two custom-made elliptical mirrors.
- Spiegel 400-750nm - € 213.00
  This is a square mirror we mounted on a retractable platform such that we could move the mirror in between the cavity mirrors to look at the alignment beam. This was an attempt to more accurately align the M2 mirror before bonding it. Unfortunately, this method proved to be too inaccurate.
- Diamond lapping sheets - € 566.05
  These are used to polish the ferrule holder, the ferrule and the fibre after everything is bonded together. This way, it is possible to achieve an optically smooth, uniform surface for the fibre-mounted assemblies.
- “Masterbond Spezialkleber” - € 3,641.15
  These were the two types of adhesive we bought from Masterbond – one with high viscosity, one with low viscosity. The latter one we used for bonding the fibre-coupled assemblies. The former one we used in the cryogenic tests, but the high-viscosity adhesive Hysol 9361 turned out to be better suited for our purposes and easier to handle.

- "Solid spacer" – € 8,506.80

  These are the fused-silica spacers for our optical setup. These spacers are bonded to the SiC bench, and the optical components (like the cavity mirrors) are bonded to the spacers.
- "Solide Ferrule Holder Bohrung" - € 1,575.00

  One of the types of elements in the "Solid spacer" order above were the elements to be used as ferrule holders. The company was not sure at first whether they would be able to drill the holes (for the ferrules) in these elements with sufficiently high accuracy. For that reason, we ordered the items without the holes for the ferrules in order to find a company to drill these holes. It turned out that the company that made the "solid spacers" would also be able to drill the holes for the ferrules with the accuracy required. Of course, this required additional work, and this cost item reflects that work for drilling the holes for the ferrules in the ferrule holders.

Travel costs

The travel costs are for scientific collaborations with ESA and cooperation partners, and for scientific dissemination at workshops and conferences. In addition to that, this includes travel costs for the commuting of the PI between Vienna and Ljubljana to enable him to continue working on the present project in the laboratory in Vienna.

6. Specific conditions and requirements

There were two conditions before the contract for the project could be signed. These conditions were fulfilled before the project started. There were no other conditions and requirements that had to be met.

7. Reportable incident

As we discussed in previous sections, we reported some changes to the funding agency. In particular, the budget reserved to the cooperation with ADS was reallocated to other parts of the project.

We described in earlier sections that the workload on the PI had to be reduced in order to accommodate his management of the FFG project QuantumShield, and to accommodate his obligations as a professor in Ljubljana.

8. References

[1] R. Kaltenbaek *et al.*, Experimental Astronomy **34**, 123 (2012).
[2] R. Kaltenbaek *et al.*, EPJ Quantum Technology **3**, 5 (2016).
[3] E. J. Elliffe *et al.*, Classical and Quantum Gravity **22**, S257 (2005).
[4] L. d'Arcio *et al.*, in *International Conference on Space Optics — ICSO 2012* (International Society for Optics and Photonics, 2017), p. 105640I.
[5] M. Armano *et al.*, Classical and Quantum Gravity **26**, 094001 (2009).
[6] L. Lindegren *et al.*, Proceedings of the International Astronomical Union **3**, 217 (2008).
[7] V. A. A. Veggel, (2007).
[8] J. Bogenstahl, Interferometry for the Space Mission LISA Pathfinder, PhD thesis, University of Glasgow, 2010.
[9] H. Kaneda *et al.*, Appl. Opt., AO **49**, 3941 (2010).

[10] A. A. van Veggel and H. Nijmeijer, Precision Engineering **33**, 7 (2009).
[11] A.-M. A. van Veggel, Philosophical Transactions of the Royal Society A: Mathematical, Physical and Engineering Sciences **376**, 20170281 (2018).
[12] A. Taylor, Aspects of Optical Meterology Systems for Space-Borne Gravitational Wave Detectors, PhD, University of Glasgow, 2014.
[13] A. Pilan Zanoni *et al.*, Applied Thermal Engineering **107**, 689 (2016).